C.P. No. 623

C.P. No. 623

MINISTRY OF AVIATION

AERONAUTICAL RESEARCH COUNCIL

CURRENT PAPERS

The Estimation of Oscillatory Wing and Control Derivatives

By

W.E.A. Acum and H.C. Garner

Aerodynamics Division, N.P.L.

LONDON: HER MAJESTY'S STATIONERY OFFICE

1964

Price 7s. 6d. net

C.P. No.623

The Estimation of Oscillatory Wing and Control Derivatives

- By -
W. E. A. Acum and H. C. Garner,
of the Aerodynamics Division,
National Physical Laboratory

March, 1961

SUMMARY

The equations arising in the lifting-surface theory of oscillating wings are reviewed briefly. The accuracy with which the theory can predict the derivatives for wings and controls oscillating in simple modes is discussed and illustrated by reference to recent experimental work at Mach numbers between 0 and 2.5.

For wings of moderate aspect ratio the agreement between theory and experiment is good in purely subsonic flow. In the upper subsonic speed range the differences between calculated and measured pitching derivatives show signs of systematic variation even when they are not small.

For slender wings at small mean incidence theoretical predictions agree surprisingly well with the few experimental data available; these show significant increases in pitching damping as mean incidence is increased.

In supersonic flow the accuracy of linearized theory is well supported by experiment; nevertheless the comparison can be greatly improved, if thickness effects are included.

In the transonic flow régime theory and experiments only agree in as much as they follow the same trend with Mach number. Frequency effect becomes especially important, yet hard to correlate and predict. The best hope appears to lie in a semi-empirical method based on linearized theory; proposed theoretical work on transonic derivatives is outlined.

Finally the large effects of slotted walls on derivatives measured in wind tunnels are discussed. This is an outstanding problem of the greatest importance, since it is essential to have reliable experimental values in the transonic speed range.

List of Contents/

Replaces N.P.L. Aero.423 - A.R.C.22,760

Published with the permission of the Director, National Physical Laboratory.

List of Contents

		Page
1.	Introduction	4
2.	Symbols and Definitions	5
	2.1 Symbols	5
	2.2 Definitions of derivatives	6
3.	Theoretical Background	7
4.	Estimation of Subsonic Derivatives	10
	4.1 Wings of moderate aspect ratio	10
	4.2 Slender wings	12
5.	Estimation of Supersonic Derivatives	13
6.	The Transonic Speed Range	14
7.	Slotted-Wall Interference Problems	15
8.	Acknowledgments	15
	References 1 to 26	16

Figures/

Figures

1. Direct pitching derivatives against M for a delta wing (A = 1.5).
2. Direct pitching derivatives against M for a delta wing (A = 2).
3. Direct pitching derivatives against M for delta wings (A = 3).
4. $-m_\theta$ and $-m_{\dot\theta}$ against h for delta wings (A = 3) at M = 0.8.
5. Direct pitching derivatives against M for a swept wing ($\Lambda_L = 33.7°$).
6. Direct pitching derivatives against M for a swept wing ($\Lambda_L = 49.4°$).
7. Direct pitching derivatives against M for a swept wing ($\Lambda_L = 59.0°$).
8. Lift and moment derivatives against h for a pitching M-wing (M = 0.8).
9. Damping derivative against M for an M-wing in a bending mode.
10. Hinge-moment derivatives against M for a delta wing (A = 1.8) with oscillating flap.
11. $-m_{\dot\theta}$ against h for a triangular wing (A = 1) at M = 0.
12. $-m_{\dot\theta}$ against h for gothic wings (A = 0.75) at M = 0.
13. $-m_\theta$ and $-m_{\dot\theta}$ against h for thick tapered wing at M = $\sqrt{2}$.
14. $-m_{\dot\theta}$ against side-edge rake for different spans of wing at M = $\sqrt{2}$.
15. $-m_\theta$ and $-m_{\dot\theta}$ against M for thick tapered wing.
16. Incremental thickness corrections to $-m_{\dot\theta}$ for wing with 5% double-wedge section.
17. $-m_{\dot\theta}$ against M for rectangular wing (A = 2) with h = 0.42.
18. $-m_\theta$ against M for rectangular wing (A = 2) with h = 0.42.
19. $-m_{\dot\theta}$ against M for a triangular wing (A = 1.5) oscillating about the half-root-chord axis.
20. Effect of slot width and spacing on derivatives measured in a slotted-wall rectangular tunnel.
21. Critical frequency for resonance in rectangular tunnels with longitudinally slotted roofs and floors.

---

1. Introduction

It is clearly important to have reliable estimates of the oscillatory derivatives of wings and control surfaces. This paper is primarily concerned with the comparison between theory and experiment for simple configurations. Experimental techniques of derivative measurement will not be discussed as the principles and details of these are described in Ref. 1. Only the basic equations of theory are given (Section 3), as the details of mathematical treatment are available in the literature. Since the emphasis is on recent unpublished work carried out at the National Physical Laboratory, the comments represent the viewpoint of one laboratory rather than a survey of the whole field.

Calculation and measurement are, as in other branches of aerodynamics, complementary, since it may be possible to apply both or only one to any specified configuration; but, whichever is used, it is desirable that the method should have been checked by a comprehensive correlation between theory and experiment. For example, the effects of a fuselage or nacelles are often difficult to represent theoretically, but greater confidence can be placed in the measured derivatives for a complete aircraft if those for wings alone are supported by calculation. Again, complicated distortional modes of vibration are difficult to reproduce in tunnel tests; the corresponding derivatives must therefore be calculated, but the method of calculation should have been checked against simpler experiments. Such comparisons are not likely to show exact agreement because of experimental errors and the idealizations of theory, but research has reached the stage where the agreement is often satisfactory, thought there are important exceptions which are discussed in this paper. Even so, the decision as to what values apply to any specific aircraft is often a difficult one. Fortunately great accuracy is seldom required.

Incompressible flow is regarded merely as a special case of subsonic flow and, if not included as such, it involves trivial theoretical modifications. Results in subsonic flow are discussed in Section 4; here a contrast becomes obvious between wings, for which derivatives can be predicted fairly well, and controls for which estimation is much more uncertain. Curiously enough, what few data are available for slender wings show that, provided the mean incidence is small, their derivatives are well estimated by theory.

Supersonic derivatives are treated in Section 5; unless M is too near to unity, the agreement is satisfactory, especially if thickness corrections can be included. Experimental information is lacking for M greater than 2.45, but the application of linearized theory and thickness corrections becomes easier until the region of hypersonic flow is reached. The reverse is true in the transonic régime (Section 6), where agreement is often poor and the trends of the derivatives with Mach number and frequency still require clarification. Since purely theoretical methods are unlikely to cater for shock-wave movement and boundary-layer interaction, the best hope is for a semi-empirical method based on linearized theory. A programme to establish the dependence of the linearized derivatives on frequency and Mach number is outlined.

Finally Section 7 considers a difficulty which has arisen recently from measurements in slotted-wall tunnels. It has been found that derivatives in subsonic and transonic flow may be sensitive to variations in slot width or

spacing./

spacing. Calculation shows that this phenomenon is not due to tunnel resonance. This outstanding problem is of crucial importance at present, since it is essential to have reliable experimental values in the transonic speed range.

2. Symbols and Definitions

2.1 Symbols

A	aspect ratio of wing ($= 2s/\bar{c}$)
B	breadth of rectangular tunnel
$b_{\phi}^{\bullet}$	damping derivative coefficient for rigid-bending mode (Section 2.2)
$\bar{c}$	geometric mean chord of wing
$\bar{c}_f$	geometric mean chord of control
c_r	root chord of wing
c_t	tip chord of wing
d	width of slot
h	$x_c/\bar{c}$
$h_{\xi}, h_{\xi}^{\bullet}$	hinge-moment derivatives (Section 2.2)
H	height of rectangular tunnel
ℓ	non-dimensional wing loading defined in equation (6)
ℓ_p	rolling-moment derivative for steady rolling (Section 2.2)
$m_{\theta}, m_{\dot{\theta}}^{\bullet}$	direct stiffness and damping derivative coefficients for pitching oscillation (Section 2.2)
M	free-stream Mach number
N	number of slots in horizontal wall of tunnel
p	pressure
p_{∞}	free-stream pressure
s	semi-span of wing
S	area of wing planform
S_f	area of control planform
t	time
T	slotted-wall tunnel parameter in equation (12), (Section 7)
U	free-stream velocity

w/

w component of velocity in the z-direction

x,y,z rectangular co-ordinates; x in the direction of U, y to starboard across the wing, z upwards

x_o distance of pitching axis downstream of root leading edge

z_o local vertical displacement of wing from its mean position

$z_\theta, z_{\dot\theta}$ derivative coefficients for lift due to pitching (Section 2.2)

α mean incidence of wing

β $\{|1 - M^2|\}^{\frac{1}{2}}$

θ_o amplitude of pitching mode $z_o = e^{i\omega t}\theta_o(x_o - x)/\bar{c}$

Λ_L sweepback of leading edge

λ taper ratio of wing $(= c_t/c_r)$

ν frequency parameter $(= \omega\bar{c}/U)$

ξ downward angle of deflection of control

ρ free-stream density

τ thickness to chord ratio at wing root

ϕ perturbation velocity potential

ϕ_o amplitude of rigid-bending mode $z_o = e^{i\omega t}\phi_o|y|$

ω angular frequency of oscillation

2.2 Definitions of derivatives

Lift due to pitching oscillation $= -\rho U^2 S\theta_o e^{i\omega t}\{z_\theta + i\nu z_{\dot\theta}^\bullet\}$

Nose-up pitching moment due to pitching oscillation

$$= \rho U^2 S\bar{c}\theta_o e^{i\omega t}\{m_\theta + i\nu m_{\dot\theta}^\bullet\}$$

Hinge moment due to oscillatory control deflection

$$= \rho U^2 S_f \bar{c}_f \xi\{h_\xi + i\nu h_\xi^\bullet\}$$

Bending moment due to rigid-bending oscillation

$$= \rho U^2 Ss\phi_o e^{i\omega t}\{b_\phi + (i\omega s/U)b_\phi^\bullet\}$$

Rolling moment due to steady rolling with angular velocity p

$$= \rho U^2 Ss(ps/U)\ell_p$$

Hinge moment and rolling moment are defined as positive in the sense of ξ increasing and p positive respectively.

3./

3. Theoretical Background

The starting point of almost all the theories to which reference will be made in this paper is the well known differential equation for linearized compressible flow,

$$\frac{\partial^2\phi}{\partial x^2} + \frac{\partial^2\phi}{\partial y^2} + \frac{\partial^2\phi}{\partial z^2} = M^2 \left\{ \frac{\partial^2\phi}{\partial x^2} + \frac{2}{U}\frac{\partial^2\phi}{\partial x \partial t} + \frac{1}{U^2}\frac{\partial^2\phi}{\partial t^2} \right\}, \qquad \ldots (1)$$

where ϕ is the perturbation velocity potential, U is the free-stream velocity in the direction of x increasing, and the wing is supposed to be thin and to remain near the plane $z = 0$ throughout its motion. The basic assumption is that only the first-order disturbances caused by the wing are significant. Equation (1) has to be solved subject to the boundary conditions, that

$$\left(\frac{\partial\phi}{\partial z}\right)_{z=0} = U\frac{\partial z_o}{\partial x} + \frac{\partial z_o}{\partial t} \qquad \ldots (2)$$

in the area bounded by the wing planform, where the wing satisfies

$$z = z_o(x,y,t) ,$$

and that the disturbances die away at infinity like outgoing waves. The pressure is then given by

$$\frac{p - p_\infty}{\frac{1}{2}\rho U^2} = -\frac{2}{U^2}\left\{ U\frac{\partial\phi}{\partial x} + \frac{\partial\phi}{\partial t} \right\}. \qquad \ldots (3)$$

In the wake p must be continuous across the plane $z = 0$, so that

$$U\frac{\partial\phi}{\partial x} + \frac{\partial\phi}{\partial t} = 0 , \qquad \ldots (4)$$

elsewhere off the wing, $\phi = 0$ in the plane $z = 0$, Further ϕ is antisymmetrical with respect to $z = 0$.

In the paper attention will be confined to oscillatory motions for which z_o in equation (2), and therefore ϕ, vary sinusoidally in time and contain a factor $e^{i\omega t}$. There is no practicable method of solving the equation for general planforms when $M < 1$, and recourse must usually be made to the numerical solution of integral equations. If $M > 1$, solutions of equation (1) can be obtained for some special planforms, but for general planforms the solution is obtained from integrals or integral equations.

For $M < 1$, ϕ may be regarded as the potential due to a distribution of doublets over the plane $z = 0$, and it may be shown that

$\phi(x,y,z)$/

$$\phi(x,y,z) = -\frac{1}{2\pi}\iint_{S+W}\phi(x',y',+0)\times$$

$$\times\frac{\partial}{\partial z}\left\{\exp\left(\frac{i\omega M^2(x-x')}{U\beta^2}\right)\exp\left(-\frac{i\omega MR}{U\beta^2}\right)\frac{1}{R}\right\}dx'dy' , \quad \ldots (5)$$

where $$R = [(x-x')^2 + \beta^2(y-y')^2 + \beta^2 z^2]^{\frac{1}{2}}$$

and the integral is taken over the wing and the wake. The required integral equation is obtained by differentiating equation (5) with respect to z. An alternative integral equation is obtained in terms of the non-dimensional loading

$$\ell = \frac{p(x,y,-0) - p(x,y,+0)}{\frac{1}{2}\rho U^2} , \quad \ldots (6)$$

where p is defined in equation (3). Then

$$\phi(x,y,z) = -\frac{U}{8\pi}\iint_{S}\ell(x',y')\exp\left(-\frac{i\omega(x-x')}{U}\right)\times$$

$$\times\int_{-\infty}^{x-x'}\exp\left(\frac{i\omega\xi}{U\beta^2}\right)\frac{\partial}{\partial z}\left\{\exp\left(-\frac{i\omega MR_o}{U\beta^2}\right)\frac{1}{R_o}\right\}d\xi dx'dy' , \quad \ldots (7)$$

where $$R_o = [\xi^2 + \beta^2(y-y')^2 + \beta^2 x^2]^{\frac{1}{2}}.$$

and, since ℓ is zero in the wake, the integration is over the wing planform only.

Equations (5) and (7) form the basis of most subsonic oscillatory wing theory. They are usually solved by the "collocation" or "kernel function" method which consists essentially in assuming for $\phi(x',y',+0)$ or ℓ a linear expression containing a number of unknown constants, then integrating to obtain $(\partial\phi/\partial z)_{z=0}$ at the same number of selected points on the planform, and finally by equation (2) solving the resulting simultaneous equations to determine the constants. Refs. 2 and 3 provide examples of this method, but there are many others as there is considerable scope for variations in numerical analysis. The methods most familiar to the authors are the extension of Multhopp's steady lifting surface theory (Ref. 4) to low frequency oscillations (Ref. 5) and to finite frequency oscillations (Ref. 6); unless otherwise stated in Figs. 1 to 12 and 17 to 19 "theory" for $M < 1$ refers to one of these methods.

Turning now to supersonic flow, we find that, although solution of the differential equations has been more successful (Ref. 7), integration methods will still be necessary for general planforms. The supersonic analogue of equation (5), derived in Ref. 8 for example, is

$w(x,y)/$

$$w(x,y) = -\frac{1}{\pi}\lim_{z\to 0}\frac{\partial^2}{\partial z^2}\iint_{S_1}\phi(x',y')\exp\left(-\frac{iM^2\omega(x-x')}{\beta^2 U}\right)\cos\left(\frac{M\omega R}{\beta^2 U}\right)\frac{1}{R}\,dx'dy', \quad \ldots (8)$$

$$R = [(x-x')^2 - \beta^2(y-y')^2 - \beta^2 z^2]^{\frac{1}{2}}$$

and the region S_1 consists of those points (x',y') for which R is real.

The analogue of equation (7), discussed in Ref. 9, is

$$w(x,y) = -\frac{U}{4\pi}\lim_{z\to 0}\iint_{S_1} \ell(x',y')\exp\left(-\frac{i\omega(x-x')}{U}\right)\times$$

$$\times\int_{\xi=\beta r}^{x-x'}\exp\left(-\frac{i\omega\xi}{\beta^2 U}\right)\frac{\partial^2}{\partial z^2}\left\{\cos\left(\frac{M\omega\sqrt{\xi^2-\beta^2 r^2}}{U\beta^2}\right)\frac{1}{\sqrt{\xi^2-\beta^2 r^2}}\right\}d\xi\,dx'dy', \quad \ldots (9)$$

where $$r = [(y-y')^2 + z^2]^{\frac{1}{2}}.$$

There is in supersonic flow an additional relation, derived by Garrick and Rubinow (Ref. 10),

$$\phi(x,y,z) = -\frac{1}{\pi}\iint_{S_1}\frac{\partial\phi}{\partial z}(x',y',0)\exp\left(-\frac{iM^2\omega(x-x')}{\beta^2 U}\right)\cos\left(\frac{M\omega R}{\beta^2 U}\right)\frac{1}{R}\,dx'dy\,, \quad \ldots (10)$$

where R and S_1 are defined below equation (8). If all the edges of the planform are supersonic, equation (10) allows the potential distribution to be determined merely by integration. Stewartson (Ref. 11) has derived modified forms to cope with planforms having leading edges which are partly subsonic.

Solutions in the form of expansions in powers of frequency parameter have been obtained for the triangular and rectangular planforms, e.g., Refs. 12 and 13. These are convenient for calculation unless M is too near unity or the frequency is high.

Theoretically equations (8), (9) and (10) and the solutions last mentioned are sufficient to provide the means of solving for almost any planform likely to be encountered in practice, but for low supersonic Mach numbers the numerical work involved is likely to be very heavy. Some possible procedures are discussed in Ref. 14; the main problem is in the field of computer programming. For these low Mach numbers (Miles (Ref. 7) has considered the slender delta planform for which the solution of Ref. 13 is also still available provided the frequency is low. Miles (Ref. 15) has also obtained a solution for the rectangular wing of low effective aspect ratio βA.

For $M = 1$ no general method exists, although Mangler (Ref. 16) and Miles (Ref. 15) have given solutions for the triangular and rectangular wings respectively. Landahl (Ref. 17) has argued that not only for $M = 1$ but for M near to unity equation (1) should be replaced by

$$\frac{\partial^2\phi}{\partial y^2}\,/$$

$$\frac{\partial^2\phi}{\partial y^2} + \frac{\partial^2\phi}{\partial z^2} = 2\frac{M^2}{U}\frac{\partial^2\phi}{\partial x \partial t} + \frac{M^2}{U^2}\frac{\partial^2\phi}{\partial t^2}\ ; \qquad \ldots (11)$$

he has given or indicated solutions for fairly general planforms.

It is also possible to solve by collocation methods the integral equation obtained by taking the limit of equation (7) as M tends to one from below (Ref. 18), and solutions have in fact been obtained by Dr. D. E. Davies at the Royal Aircraft Establishment.

One must also mention two methods applicable in very restricted fields, namely unsteady slender-wing theory, e.g., Ref. 19, for wings of exceedingly small aspect ratio, and piston theory (Ref. 20) for high supersonic Mach numbers only. The second of these includes thickness effects which are discussed in Section 5.

The conditions under which the various differential equations of flow are applicable have been analysed by Miles (Ref. 7) and Landahl (Ref. 21). Ref. 7 gives a full treatment of the equations of unsteady supersonic flow and a general mathematical account of the subject.

4. Estimation of Subsonic Derivatives

4.1 Wings of moderate aspect ratio

The subsonic lifting-surface theories mentioned in the previous section may be expected to apply to wings oscillating with sufficiently small amplitude, provided that the mean flow does not violate the conditions implicit in the linearized equations. For example, if the Mach number is so high that regions of supersonic flow exist, linear perturbations in velocity cannot adequately describe the flow; again, if the wing is so slender that free vortices are shed from the leading edge, then it is no longer correct to represent the perturbed flow as that due to a vortex sheet in a plane. The accuracy of the solutions will depend on how well the wing planform and the mode of oscillation are represented by the finite number of quantities used in approximating to the integral equation.

As examples of configurations for which these considerations might lead us to expect reasonable agreement, consider the set of three delta wings of constant taper ratio $\lambda = \frac{1}{7}$ whose direct pitching derivatives about two axes are shown as functions of Mach number in Figs. 1 to 3. These experiments were performed in the N.P.L. $9\frac{1}{2}$ in. tunnel with half models having conventional aerofoil sections, 6% thick for all three planforms and also 10% thick for the aspect ratio $A = 3$. Some general trends may be observed; the experimental damping derivative, $-m'_\theta$, agrees fairly well with theory up to $M = 0.6$, but for higher values of M the experimental values tend to be lower than theory for the forward axis and higher than theory for the rearward axis. The experimental stiffness derivative, $-m_\theta$, for the forward axis is in good agreement with theory up to $M = 0.6$; at higher values of M the experimental values for both axes are consistently of lower magnitude than that obtained theoretically. These trends with axis position are indicated in Fig. 4 for $M = 0.8$.

The same remarks apply to the set of three swept wings of constant aspect ratio $A = 2.64$ and taper ratio $\lambda = \frac{7}{18}$ for which derivatives are

shown/

shown in Figs. 5 to 7. These experimental values were also obtained in the N.P.L. $9\frac{1}{2}$ in. tunnel with half-models of conventional aerofoil section, 6% thick. Other details of the comparisons are remarkably consistent for all six wings. The measured values of $-m_{\dot{\theta}}$ for the forward axis are constant or fall initially with Mach number, but above $M = 0.8$ they rise to a peak value (usually below theory) which flattens with increasing sweepback. While the measured values of $-m_{\dot{\theta}}$ for the rearward axis agree well with theory at $M = 0.6$ and $M = 0.9$ in all cases, the intermediate experimental values are up to 40% above theory. There is little calculated or measured effect of M on $-m_{\theta}$ for the rearward axis, the experimental value being 10% to 20% low numerically in each case. Such comparisons are encouraging since the differences show signs of systematic variation even when they are not small and provide a promising basis for estimating subsonic pitching derivatives.

Derivatives for a much less conventional M-wing planform are shown in Fig. 8, and these include the theoretical effect of finite frequency (Ref. 22) as calculated by Ref. 6, as well as derivatives for low frequency, but unfortunately model flexibility restricted measurement of the derivatives to low frequency parameters. The measurements (Ref. 23) were made in the N.P.L. 25 in. by 20 in. tunnel with slotted roof and floor and included lift and moment derivatives, the latter for three pitching axes. In Fig. 8 the four derivatives are plotted against axis position for $M = 0.8$. When the tests were repeated with the roof and floor completely closed, experimental discrepancies were revealed of magnitude comparable to that predicted in Ref. 22 for a frequency change from $\nu = 0$ to $\nu = 0.6$. Since the experimental frequency parameter is low, corrections to the closed-tunnel in-phase derivatives may be made by steady tunnel-interference theory; this does in fact improve the agreement for $-z_{\theta}$ and $-m_{\theta}$. Unfortunately no simple method of correcting the out-of-phase derivatives appears to be available; however, the two experimental values of $-z_{\dot{\theta}}$ and $-m_{\dot{\theta}}$ lie on opposite sides of the theoretical curves. The problem of slotted-wall interference is discussed in Section 7.

In spite of these reservations the picture for wings of moderate aspect ratio in rigid pitching at Mach numbers well below unity is fairly encouraging. It is now necessary to consider some other modes. Fig. 9 shows the direct damping derivative for a half model of the same M-wing planform treated in Fig. 8, in a rotational oscillation about a streamwise axis just outside the tunnel wall. This rigid-bending mode thus corresponds to a flapping motion with a small amount of vertical translation superimposed. The agreement in this case is very good for the range of Mach number $0.6 \leq M \leq 0.8$ for which both theoretical and experimental results are available. Since the derivative $-b_{\dot{\phi}}$ might be expected to have characteristics similar to those of the steady rolling derivative, $-\ell_p$, the theoretical curve for the latter is also plotted and is expected to be a reliable estimate. It must be added, however, that half-model tests of rectangular wings of aspect ratio 2 and 4 gave less satisfactory agreement, especially for $A = 2$.

The evidence for rigid pitching leads one to expect that, provided a mode involving deformation has a simple shape, theory could predict its derivatives fairly well; but, as deforming modes are difficult to produce in a wind tunnel, this point cannot be regarded as proved. Modes which involve

discontinuities/

discontinuities in the slope of the wing may be expected to cause difficulty, unless special precautions are taken. The commonest example is that of a trailing-edge control where discontinuous downwash is required at the hinge line. The disposition of the collocation points relative to the hinge line could have a large effect on the calculated lift distribution. One way of overcoming this difficulty is to replace the wing by a continuously deforming surface chosen so that each chordwise section, when treated by two-dimensional theory, has the correct lift pitching moment and hinge moment. Obviously this procedure is not ideal, but, as Fig. 10 shows, it can give results for the hinge-moment damping derivative, $-h'_{\xi}$, in good agreement with experiment; low experimental values of the stiffness derivative, $-h_{\xi}$, are to be expected from the boundary-layer effects that occur in steady flow. It should also be noted that some control derivatives, for example overall lift due to control oscillation, may be calculated by using the reverse-flow theorem (Ref. 24).

In most of this section so far the frequency parameters of the experiments have been low, and in fact data on the derivatives at high values are scanty and confused except for low speeds where frequency effects in any case tend to be small. Otherwise the frequency effects shown by theory and experiment sometimes agree and sometimes disagree; in the latter case experimental scatter may be of the same magnitude as the theoretically predicted frequency effect.

4.2 Slender wings

In the development of the linearized theory it is assumed that all the vorticity in the flow is confined to a nearly plane region extending downstream of the leading edge of the wing, and also that the perturbation velocity is everywhere small. As is well known, the flow round wings with slender planforms, especially those with sharp leading edges, may contain concentrated free vorticity so that these assumptions are not fulfilled. It might therefore be expected that linearized theory would be inaccurate for such wings, and that a new theory would have to be developed to include the effect of the free vorticity, but the data in Figs. 11 and 12 show that this is not necessarily true.

Calculations for a triangular wing of aspect ratio 1.0 and a gothic wing of aspect ratio 0.75 have been compared with measurements of pitching damping at low speeds; the results are plotted against axis position h in Figs. 11 and 12 respectively. Although the models have sharp leading edges, the derivative $-m'_{\theta}$ for small oscillations about zero mean incidence ($\alpha = 0$) lies very close to the value given by lifting-surface theory. The results afford experimental confirmation of the deficiencies of slender-wing theory, which often exceed 50%, even for such low aspect ratios. Preliminary unconfirmed measurements on the triangular wing made at the Royal Aircraft Establishment, Bedford, corroborate those made by Bristol Aircraft Ltd., both as regards the special case $\alpha = 0$ and the trend with increasing mean incidence (Fig. 11). Fig. 12 for the gothic wing not only shows the same trend with increasing mean incidence, but includes values of $-m'_{\theta}$ measured by Bristol Aircraft Ltd., on two models of different maximum thickness ratio, τ. It is significant that the trend towards greater damping with increasing mean incidence is also obtained with decreasing τ; each of these variations might be expected to intensify the non-linear effect of leading-edge separation.

These comparisons are encouraging as far as they go, but as they cover only two planforms and low Mach numbers, the wider question of the accuracy of theoretical prediction must await settlement until more experimental evidence is available.

5./

5. Estimation of Supersonic Derivatives

The various integral expressions quoted in Section 3 provide, formally at least, a method of calculating the forces on any wing in supersonic flow, although for low supersonic Mach numbers the large number of intersecting Mach lines crossing the wing may present formidable problems of programming. Nevertheless considerable progress has been made in this direction, and it seems likely that in the near future most practical planforms will be amenable to calculation.

There remains the question of how well such calculations will predict the derivatives. Fig. 13 shows a fair comparison between linearized theory and experimental values of $-m_{\dot{\theta}}$ and $-m_{\theta}$ against h obtained in the N.P.L. 11 in. tunnel, for a tapered unswept planform at $M = \sqrt{2}$. The model used in the experiment had a sectional shape which was geometrically similar from root to tip; this was a double wedge of thickness ratio 0.05. Allowance was made for this thickness by applying van Dyke's two-dimensional oscillating aerofoil theory (Ref. 25) on a strip-theory basis. Fig. 13 shows that the thickness correction gives a large improvement in the comparison. As described in Ref. 26, the same result was found for higher Mach numbers.

Fig. 14, reproduced from Ref. 26, shows the comparisons for a family of models obtained from that of Fig. 13 by cutting off portions near the tip. These results are for $M = \sqrt{2}$ and oscillation about the mid-root-chord axis, the variable being the angle at which the tip is cut off. If the tip is removed by making a single cut normal to the planform, then a non-streamwise tip will have a leading or trailing edge of finite thickness; these cases are referred to as "blunt raked edge" and are denoted in Fig. 14 by solid circles. For some tests this blunt raked edge was machined so that the wing section was still everywhere a 5% double wedge as in the case of a streamwise tip. Reference to Fig. 14 shows that the effect of this modification can be appreciable especially when applied to the leading-edge. For the wings of the two largest spans ($s/c_r = 1.37$ and $s/c_r = 1.00$) the agreement of theory and experiment is improved by adding a thickness correction. The same is true for the smallest span ($s/c_r = 0.625$) when the tip is in the streamwise direction; for blunt raked edges and small span agreement with theory is poor, but this is not surprising since a large proportion of the wing area is affected by the blunt tips.

Some idea of the effect of varying Mach number is given by Fig. 15, which reinforces the remarks already made and also shows how the thickness correction is predicted by piston theory. At the high Mach numbers, where this may be expected to apply, the corrections are small. Fig. 16 has therefore been included to show how the thickness corrections, $-\Delta m_{\dot{\theta}}$, according to the two theories vary with Mach number; the limiting value by van Dyke's theory as M tends to infinity is in fact the value computed (formally) by piston theory for $M = 0$. Piston theory includes the thickness parameter squared whereas van Dyke's includes it linearly, so that piston theory may be more accurate for very high M.

It seems generally advantageous to apply a thickness correction unless the wing has subsonic leading edges or the equivalent aspect ratio $A\beta$ is small. For lower supersonic Mach numbers the picture is less satisfactory and only much rougher agreement can be expected.

6./

6. The Transonic Speed Range

As already stated, derivatives can be calculated without great difficulty for fairly low subsonic and fairly high supersonic Mach numbers; then the effects of frequency are seldom large. It is found, both experimentally and theoretically, that when M is near to unity the frequency effects may be large and complicated. Moreover the applicability of linearized theory is dubious owing to the possible occurrence of large regions in the flow field where the perturbation velocity is not small, and solutions of the linearized equations are not always easily obtained especially for low supersonic M. There are also, as we shall see later (Section 7), some difficulties from the experimental point of view.

It cannot, therefore, be expected that derivatives will be predicted as accurately for transonic flow as for subsonic or supersonic flow. An example of the situation which may arise is provided by Figs. 17 and 18 which give the respective pitching derivatives $-m_{\dot{\theta}}$ and $-m_{\theta}$ for a rectangular wing of aspect ratio 2.0 as functions of M. From low-frequency theories there are full curves for $M < 1$ from Ref. 5, for $M > 1$ from Ref. 12, and for low supersonic Mach numbers from Ref. 15; this last solution due to Miles may be expected to be fairly accurate in a range of Mach number up to about $M = 1.1$ for this wing. The broken curves for non-zero frequency parameters were obtained by the method of Ref. 2 for $M < 1$ and from Ref. 12 for $M > 1$. Also plotted in Figs. 17 and 18 are the two derivatives for transonic M predicted by Landahl's theory (Ref. 17, Part II); these are in good agreement with values calculated by Dr. D. E. Davies at the R.A.E., using a collocation method in the limit as $M \to 1$. The experimental points, obtained in the N.P.L. 25 in. by 20 in. tunnel, support fairly well the general trend of theory for both $-m_{\dot{\theta}}$ and $-m_{\theta}$ but differ widely in detail. The variation with frequency is probably within the experimental error except for the large changes which occur near $M = 1$, when the trend is the same as in theory although quantitatively different. The conclusion is that at present theory can only provide very rough estimates.

In Figs. 17 and 18 the theories themselves do at least indicate clearly the sign of the frequency effect near $M = 1$, but Fig. 19 for a triangular wing of aspect ratio 1.5 suggests that this is not generally true. In Fig. 19 sonic theory (Mangler, Ref, 16) predicts a variation in $m_{\dot{\theta}}$ of opposite sign to that found by linearized theory for $M = 0.99$. The collocation theory of Dr. D. E. Davies for $M = 1$ predicts the same trend as Mangler's theory but is different quantitatively. The value predicted by Landahl's theory (Ref. 21) for $\nu = 0.05$ agrees fairly well with Mangler's theory. Since according to low-frequency theory $-m_{\dot{\theta}}$ tends to $+\infty$ as $M \to 1$ from below and tends to $-\infty$ as $M \to 1$ from above, rapid changes in $-m_{\dot{\theta}}$ can be expected near $M = 1$. Evidently it is exceedingly difficult to obtain reliable theoretical curves in such cases. As for $M = 0$ in Fig. 11, simple slender-wing theory gives a value much too high for subsonic and supersonic Mach numbers.

It is intended that calculations by linear theory shall be made for the rectangular and triangular wings at non-zero frequencies and several Mach numbers in the low supersonic range $1.0 < M < 1.1$. The aim is to establish reliable transonic theoretical curves against M for fixed frequency parameters, and then to use these curves and available experimental results semi-empirically, or perhaps as a basis for more advanced non-linear theories.

7./

7. Slotted-Wall Interference Problems

In order to obtain derivatives at transonic speeds it is necessary to avoid choking the wind tunnel, and one common way of doing this is by incorporating longitudinal slots in part or all of the working section. For example, the experimental results described in Section 6 were obtained in a rectangular tunnel with solid side-walls and a slotted roof and floor. This arrangement succeeds in making transonic tests possible but introduces the complication that there is no known method of calculating the unsteady wall interference.

To investigate slotted-wall interference some measurements were made in the N.P.L. 25 in. by 20 in. tunnel using the half-model of an M-wing shown in Fig. 8 and mentioned in Section 4.1. In the normal state the roof and floor of the tunnel each have eleven slots. These were progressively sealed and the effect on the pitching derivatives observed. Fig. 20 shows how they vary with the number of slots left open. Here T is the parameter commonly used for steady slotted-wall interference, defined by

$$T = \frac{1 - \frac{B}{\pi NH} \log_e \operatorname{cosec} \frac{\pi Nd}{2B}}{1 + \frac{B}{\pi NH} \log_e \operatorname{cosec} \frac{\pi Nd}{2B}} \qquad \ldots (12)$$

where the tunnel has height H, breadth B and N slots of width d in each horizontal wall. For the closed tunnel $T = -1$, and for open roof and floor $T = +1$. Both derivatives $-m_\theta$ and $-m_{\dot{\theta}}$ vary smoothly with T; the effect on the damping derivative is found to be very large especially for the higher values of M.

This phenomenon is not due to tunnel resonance, indeed the critical resonance frequency for a slotted tunnel is higher than that for a closed tunnel. Fig. 21 shows how the critical frequency varies with the open area ratio for a tunnel having slots in its roof and floor at a spacing equal to $\frac{1}{6}$H. Calculations were made for two open area ratios by regarding the working section as a resonating cavity and calculating its fundamental frequency by the well known relaxation method.

No satisfactory explanation of variations of the derivatives with T is known. A simple empirical observation is that, as T is varied for a fixed M, the ratio of the lift vector to the moment vector in the plane of real and imaginary parts remains roughly constant. Further tests designed to facilitate a semi-empirical method of correction are to be undertaken at the N.P.L. by a series of measurements in three slotted-wall tunnels.

8. Acknowledgments

The experimental results in Figs.11 and 12 are published by kind permission of the Ministry of Aviation, Bristol Aircraft Ltd., and Mr. J. S. Thompson of the Royal Aircraft Establishment. Mrs. S. Lucas assisted with the theoretical calculations and the preparation of the figures.

References/

References

1. J. B. Bratt — Wind-tunnel techniques for the measurement of oscillatory derivatives. A.R.C. R. & M.3319. August, 1960.

2. J. R. Richardson — A method of calculating the lifting forces on wings (Unsteady subsonic and supersonic lifting surface theory). A.R.C. R. & M.3157. April, 1955.

3. C. E. Watkins, D. S. Woolston and H. J. Cunningham — A systematic kernel function procedure for determining aerodynamic forces on oscillating or steady finite wings at subsonic speeds. N.A.S.A. TR R-48. 1959

4. H. Multhopp — Method of calculating the lift distribution of wings (Subsonic lifting surface theory). A.R.C. R. & M.2884. January, 1950.

5. H. C. Garner — Multhopp's subsonic lifting surface theory of wings in slow pitching oscillations. A.R.C. R. & M.2885. July, 1952.

6. W. E. A. Acum — Theory of lifting surfaces oscillating at general frequencies in a stream of high subsonic Mach number. A.R.C.17,824. 1956. See also A.R.C.18,630 (1956); 19,229 (1957); 20,771 (1959).

7. J. W. Miles — The Potential Theory of Unsteady Supersonic Flow. Cambridge University Press, 1959.

8. W. P. Jones — Supersonic theory for oscillating wings of any planform. A.R.C. R. & M.2655. June, 1948.

9. C. E. Watkins and J. H. Berman — On the kernel function of the integral equation relating lift and downwash distributions of oscillating wings in supersonic flow. N.A.C.A. Report 1257. 1956.

10. I. E. Garrick and S. I. Rubinow — Theoretical study of air forces on an oscillating or steady thin wing in a supersonic main stream. N.A.C.A. Report 872. 1947.

11. K. Stewartson — On the linearized potential theory of unsteady supersonic motion. Part II. Quart. Jour. Mech. and Applied Math., Vol.5, p.137. 1952.

12. H. C. Nelson, Ruby A. Rainey and C. E. Watkins — Lift and moment coefficients expanded to the seventh power of the frequency for oscillating rectangular wings in supersonic flow and applied to a specific flutter problem. N.A.C.A. Tech. Note 3076. April, 1954.

13./

13. C. E. Watkins and J. H. Berman — Velocity potential and air forces associated with a triangular wing in supersonic flow, with subsonic leading edges, and deforming harmonically according to a general quadratic equation. N.A.C.A. Tech. Note 3009. September, 1953.

14. H. C. Garner and W. E. A. Acum — Proposed application of linearized theoretical formulae to general mechanized calculations for oscillating wings at supersonic speeds. N.P.L./Aero/388. August, 1959.

15. J. W. Miles — On the low aspect ratio oscillating rectangular wing in supersonic flow. Aero. Quart., Vol. 4, p.231. 1953.

16. K. W. Mangler — A method of calculating the short period longitudinal stability derivatives of a wing in linearised unsteady compressible flow. A.R.C. R. & M.2924. June, 1952.

17. M. T. Landahl — Theoretical studies of unsteady transonic flow. Parts I to V. F.F.A. (Sweden) Reports 77 to 81. 1958, 1959.

18. C. E. Watkins, H. L. Runyan and D. S. Woolston — On the kernel function of the downwash equation relating the lift and downwash distributions of oscillating finite wings in subsonic flow. N.A.C.A. Report 1234. 1955.

19. I. E. Garrick — Some research in high speed flutter. Anglo-American Aeronautical Conference, Brighton. 1951.

20. M. J. Lighthill — Oscillating airfoils at high Mach number. Jour. Aero. Sci., Vol. 20, p.402. 1953.

21. M. T. Landahl — The flow around oscillating low aspect ratio wings at transonic speeds. K.T.H. (Sweden) Aero. TN 40. 1954.

22. H. C. Garner and W. E. A. Acum — Theoretical subsonic derivatives for an oscillating M-wing. A.R.C. R. & M.3214. January, 1959.

23. J. B. Bratt and K. C. Wight — Measurements of pitching oscillation derivatives at subsonic and transonic speeds for an M-wing (Interim Report). A.R.C.21,661. February, 1960.

24. A. H. Flax — Reverse flow and variational theorems for lifting surfaces in nonstationary compressible flow. Jour. Aero. Sci., Vol. 20, p.120. 1953.

25./

25. M. D. van Dyke — Supersonic flow past oscillating airfoils including nonlinear thickness effects. N.A.C.A. Report 1183. 1954.

26. D. E. Lehrian — Calculation of stability derivatives for tapered wings of hexagonal planform oscillating in a supersonic stream. A.R.C. R. & M.3298. September, 1960.

DSD 74723 Wt.59 K4 11/63 XL & CL

FIG. 1

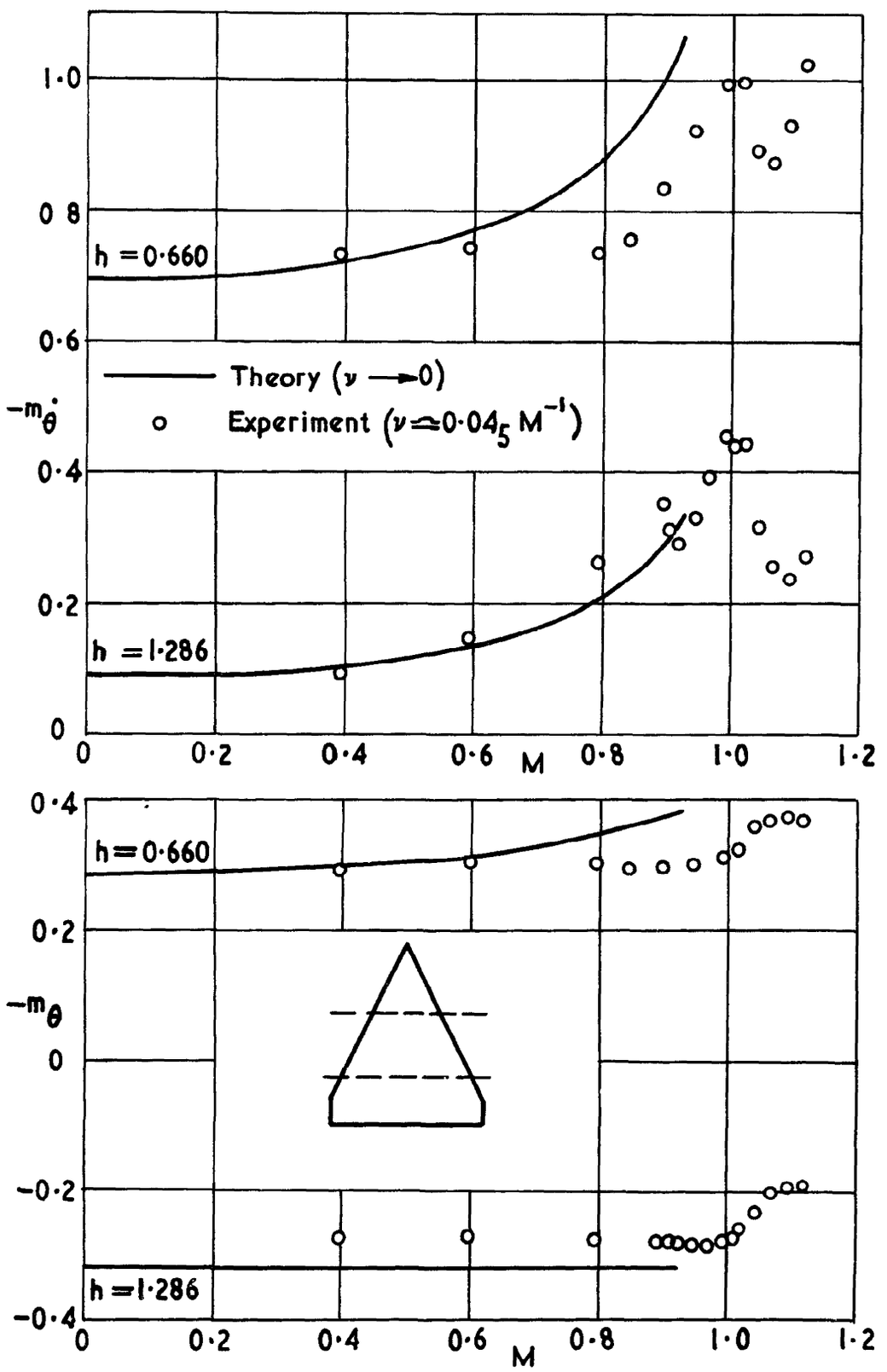

Direct pitching derivatives against M for a delta wing (A = 1·5)

FIG. 2

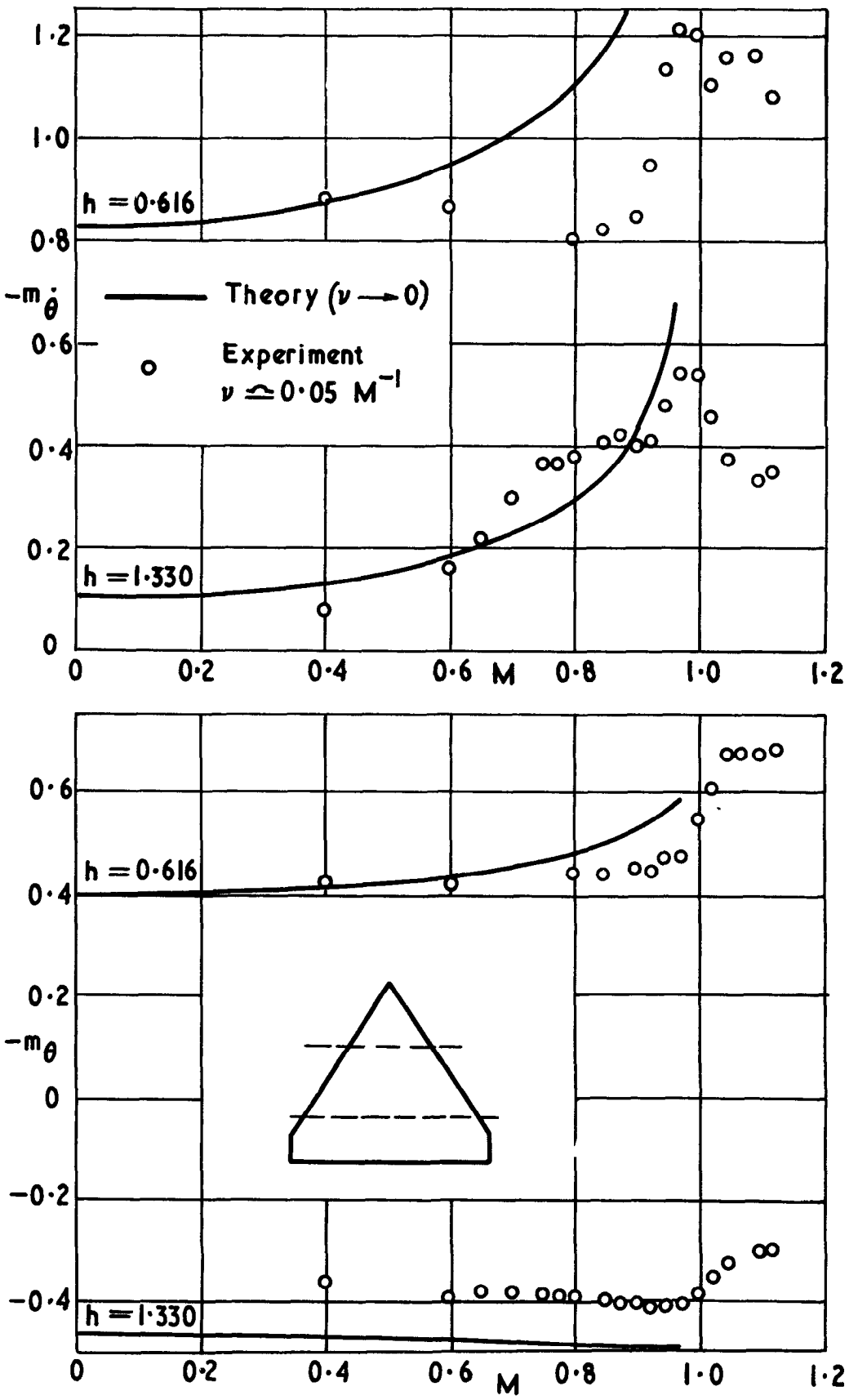

Direct pitching derivatives against M for a delta wing (A = 2)

FIG. 3

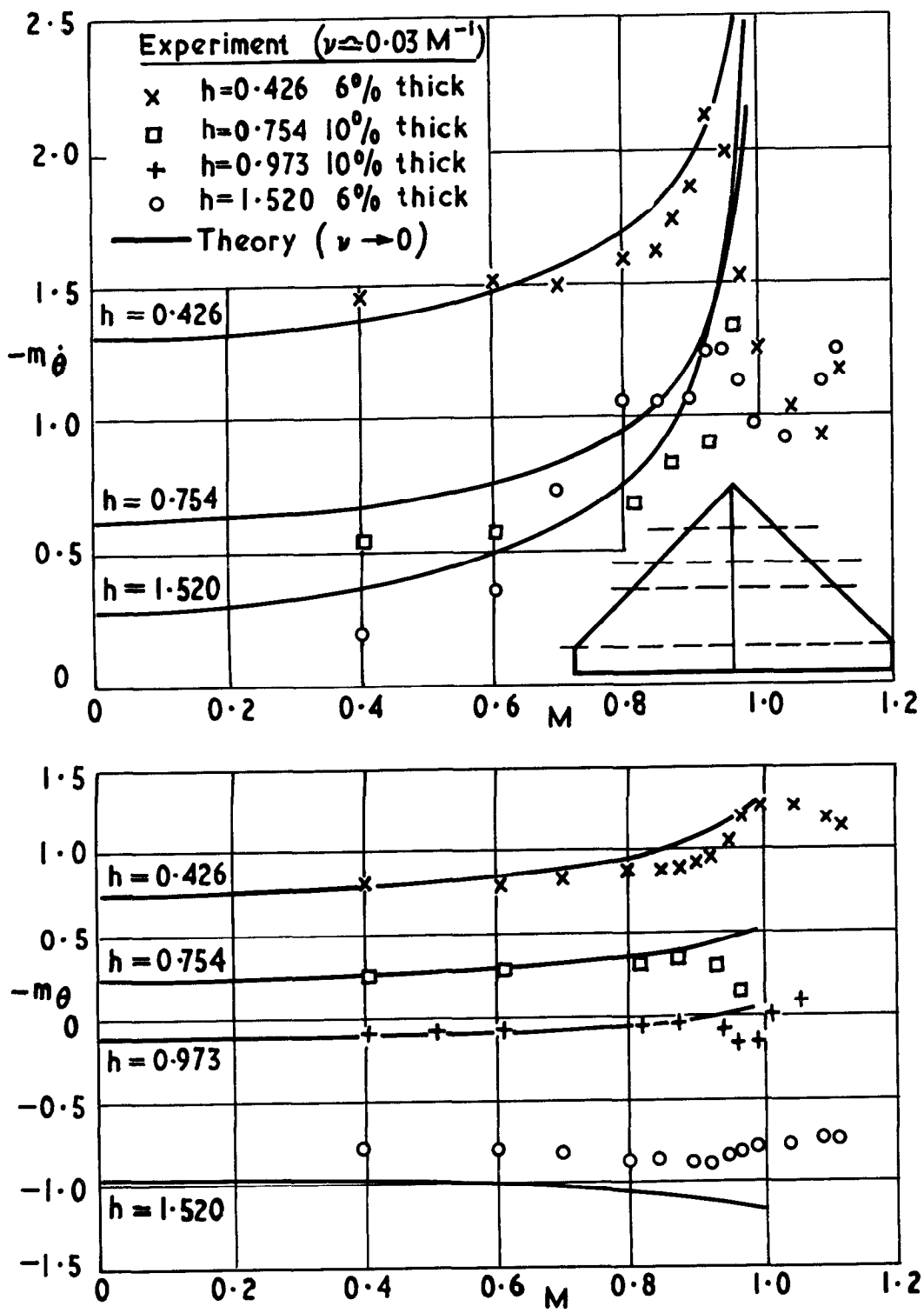

Direct pitching derivatives against M for delta wings (A = 3)

FIG. 4

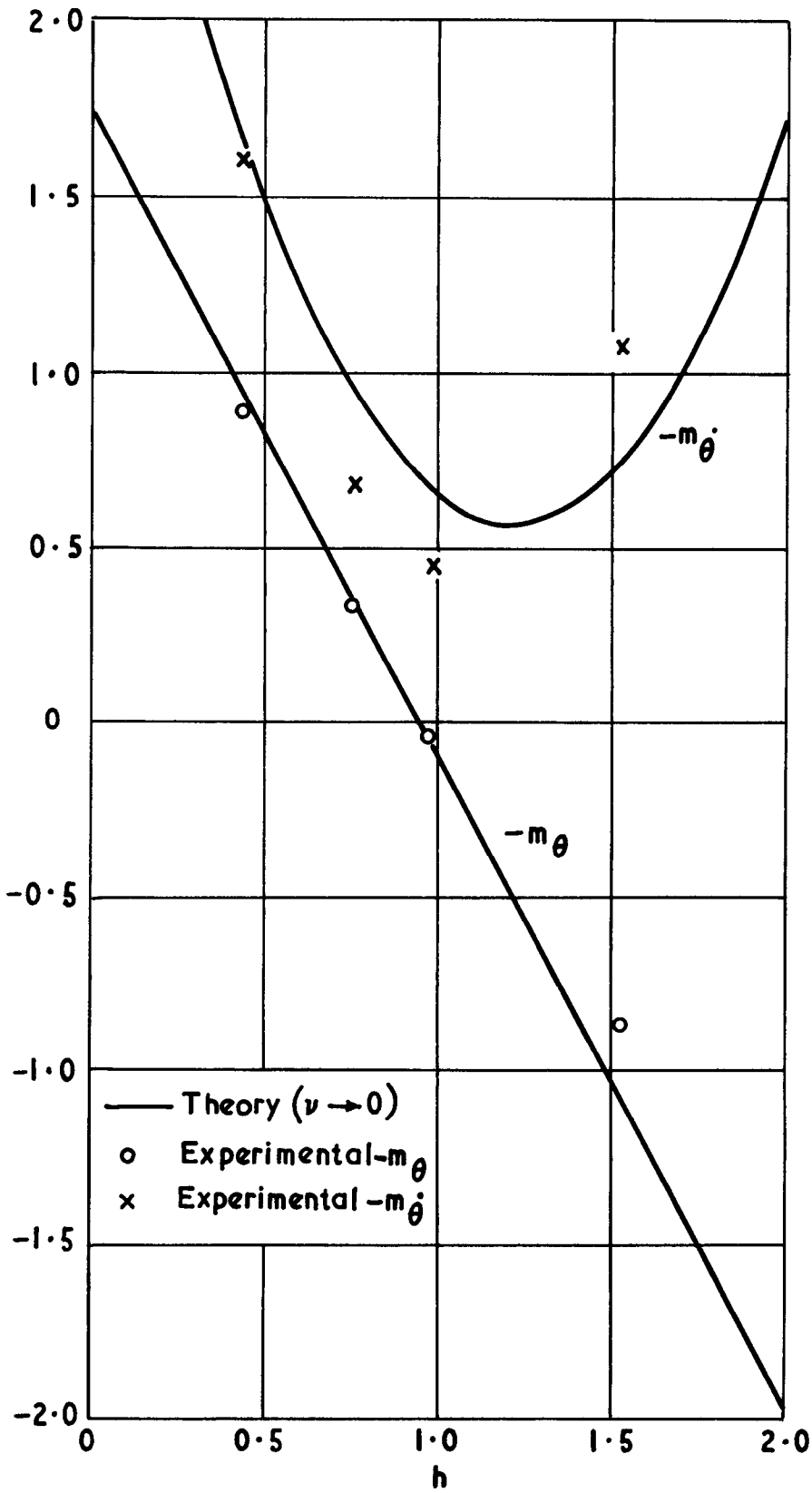

$-m_{\theta}$ and $-m_{\dot{\theta}}$ against h for delta wings (A=3) at M=0·8

FIG.5

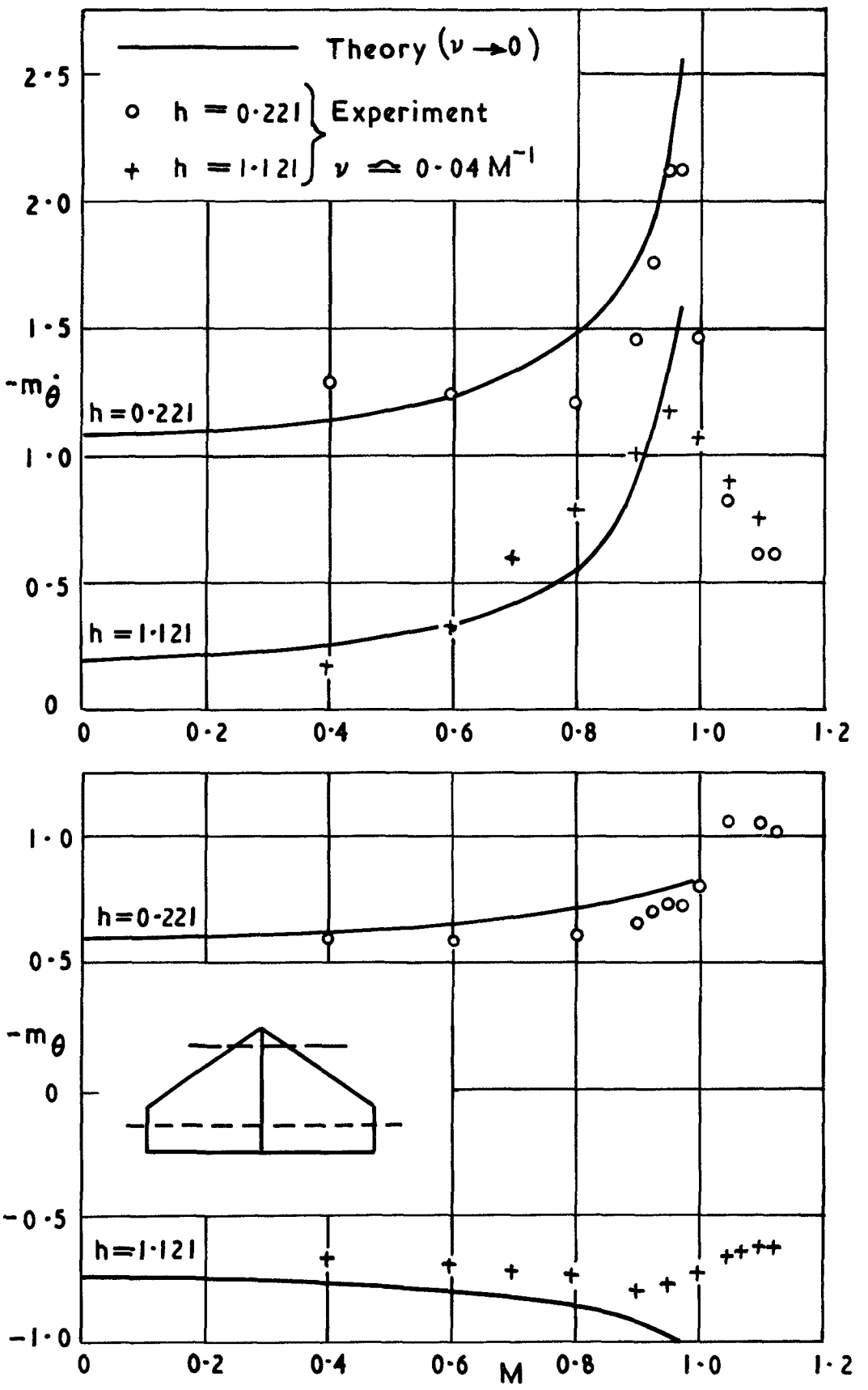

Direct pitching derivatives against M for a swept wing ($\Lambda_L = 33·7^0$)

FIG.6

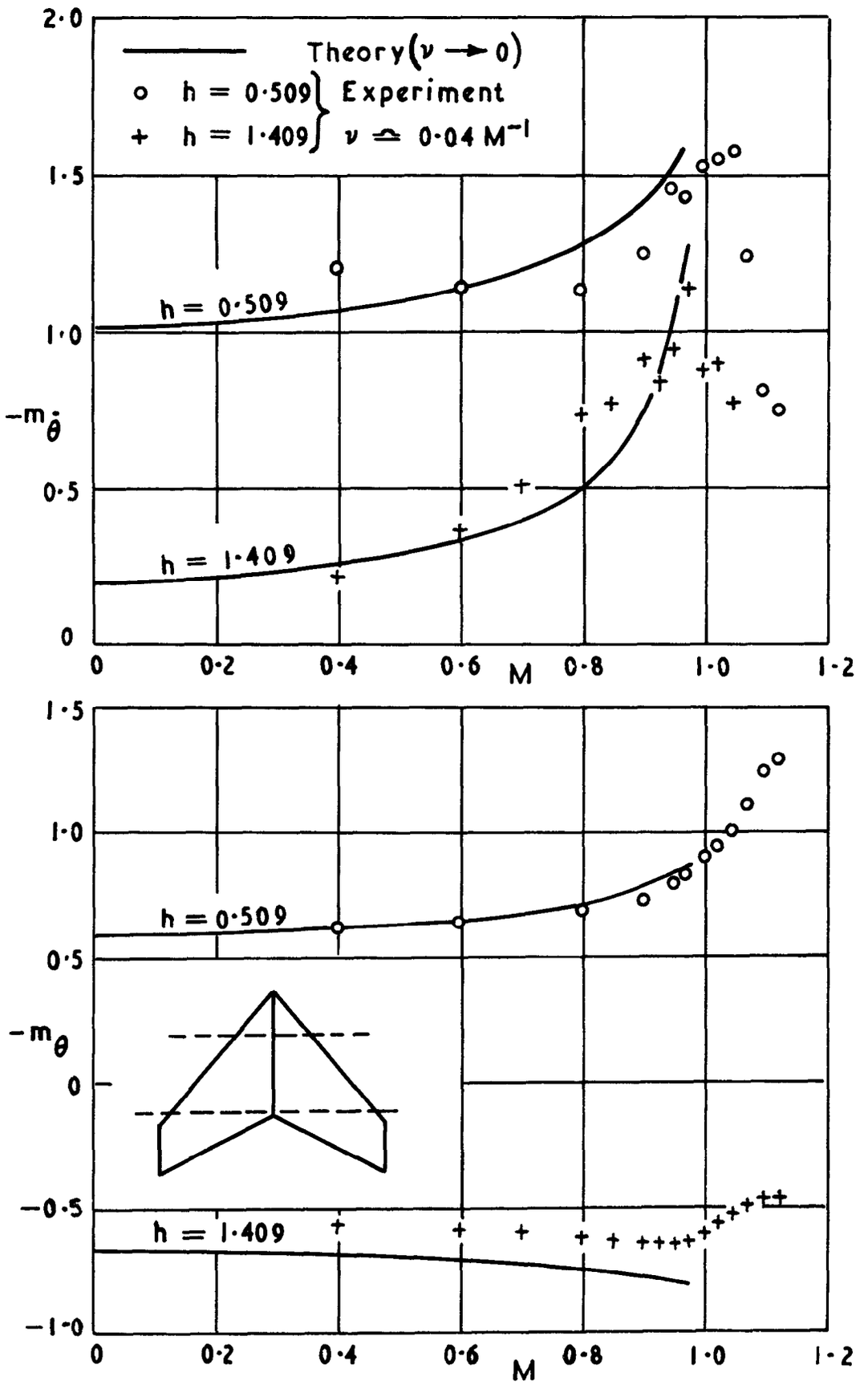

Direct pitching derivatives against M for a swept wing ($\Lambda_L = 49{\cdot}4°$)

FIG 7

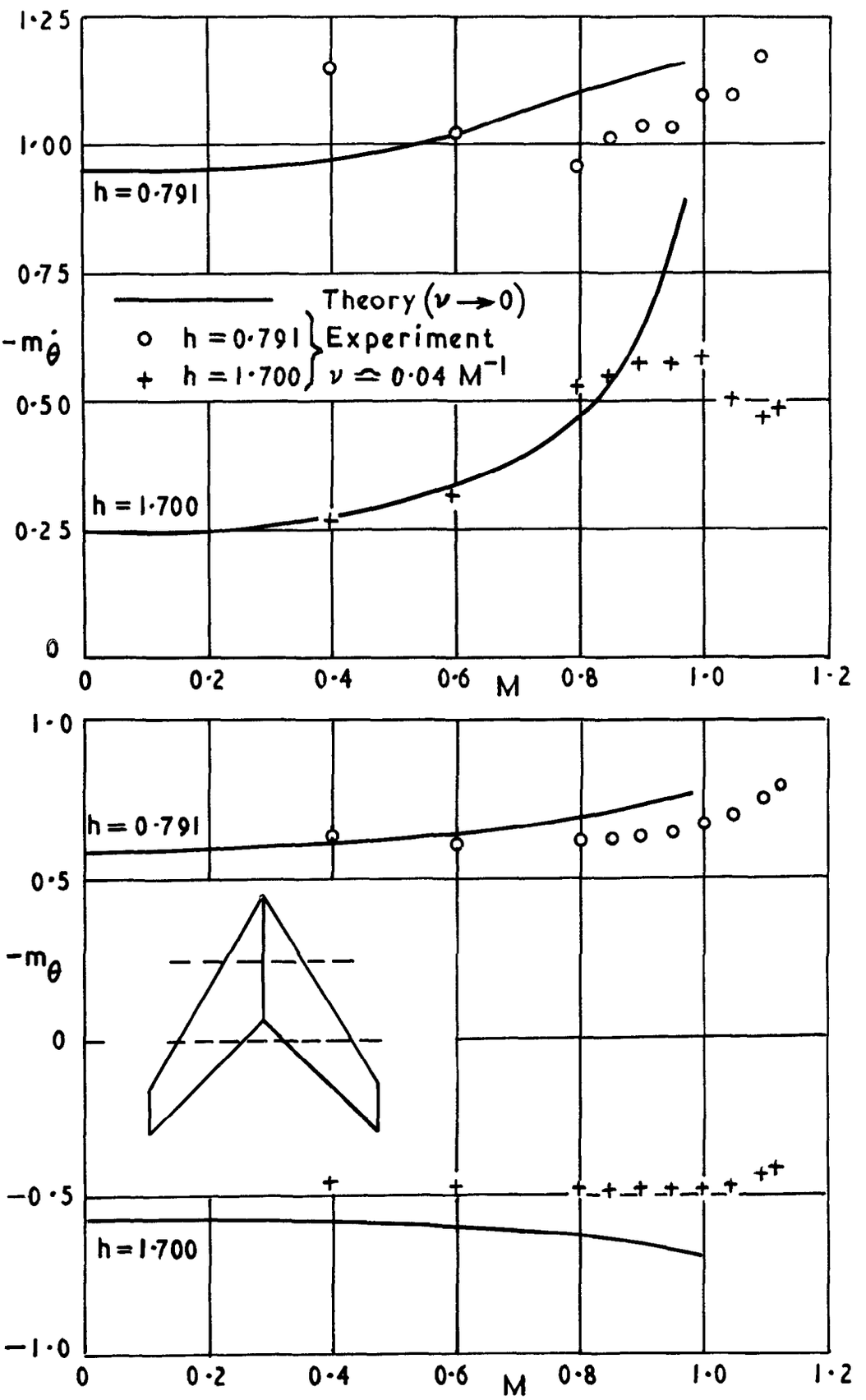

Direct pitching derivatives against M for a swept wing ($\Lambda_L = 59{\cdot}0°$)

FIG. 8

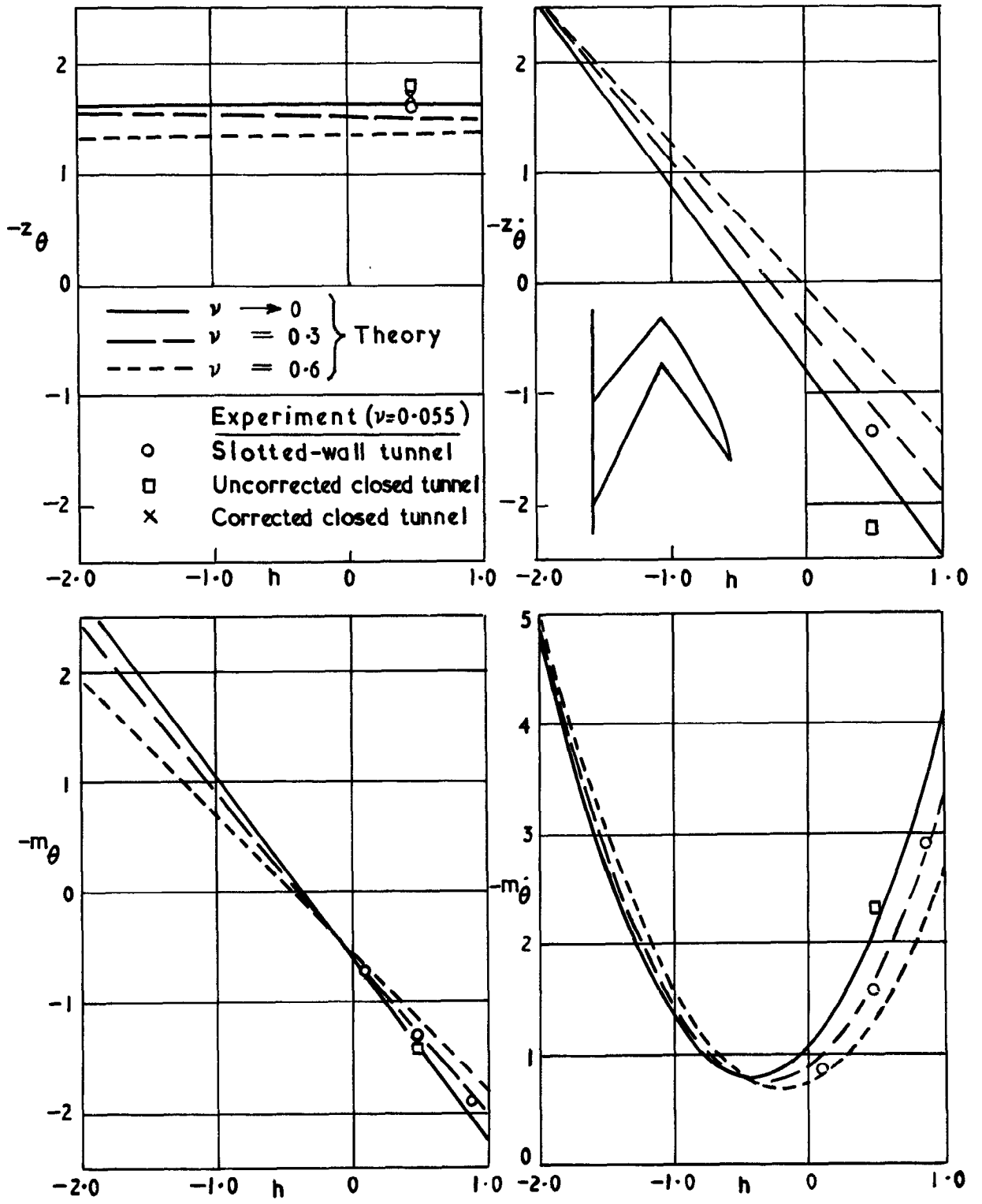

Lift and moment derivatives against h for a pitching M-wing ($M = 0{\cdot}8$)

FIG. 9

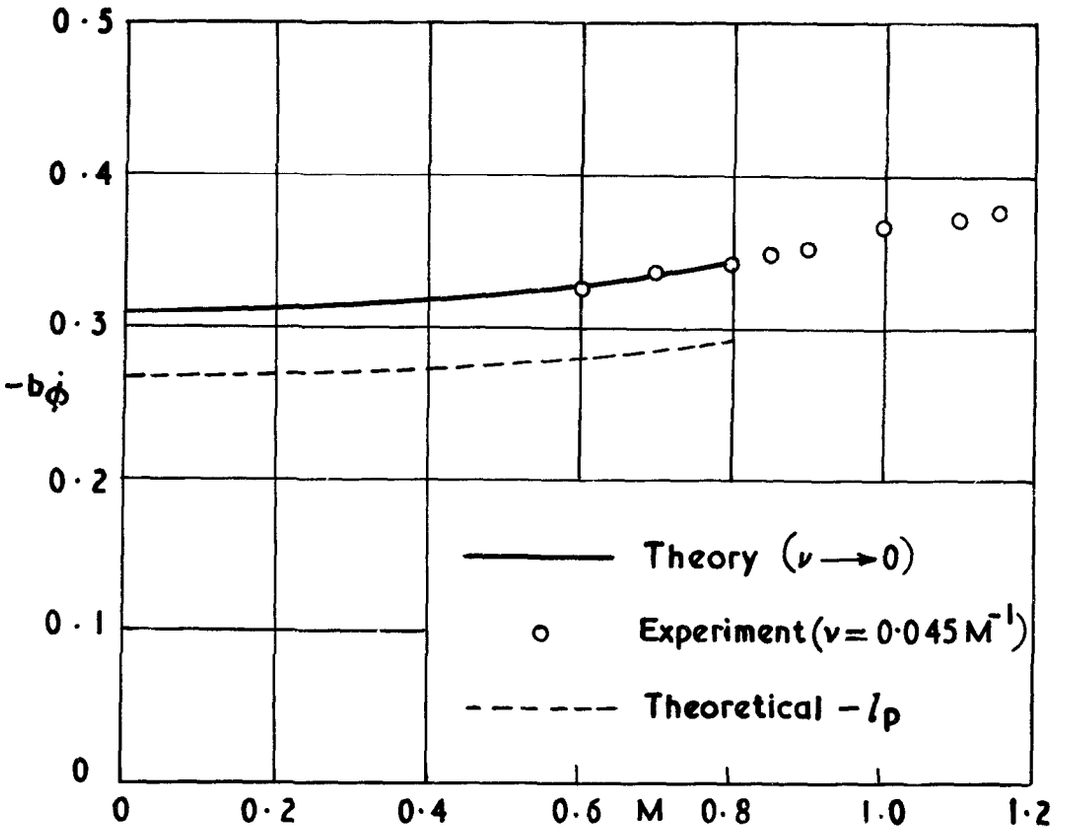

Damping derivative against M for an M-wing in a bending mode

FIG. 10

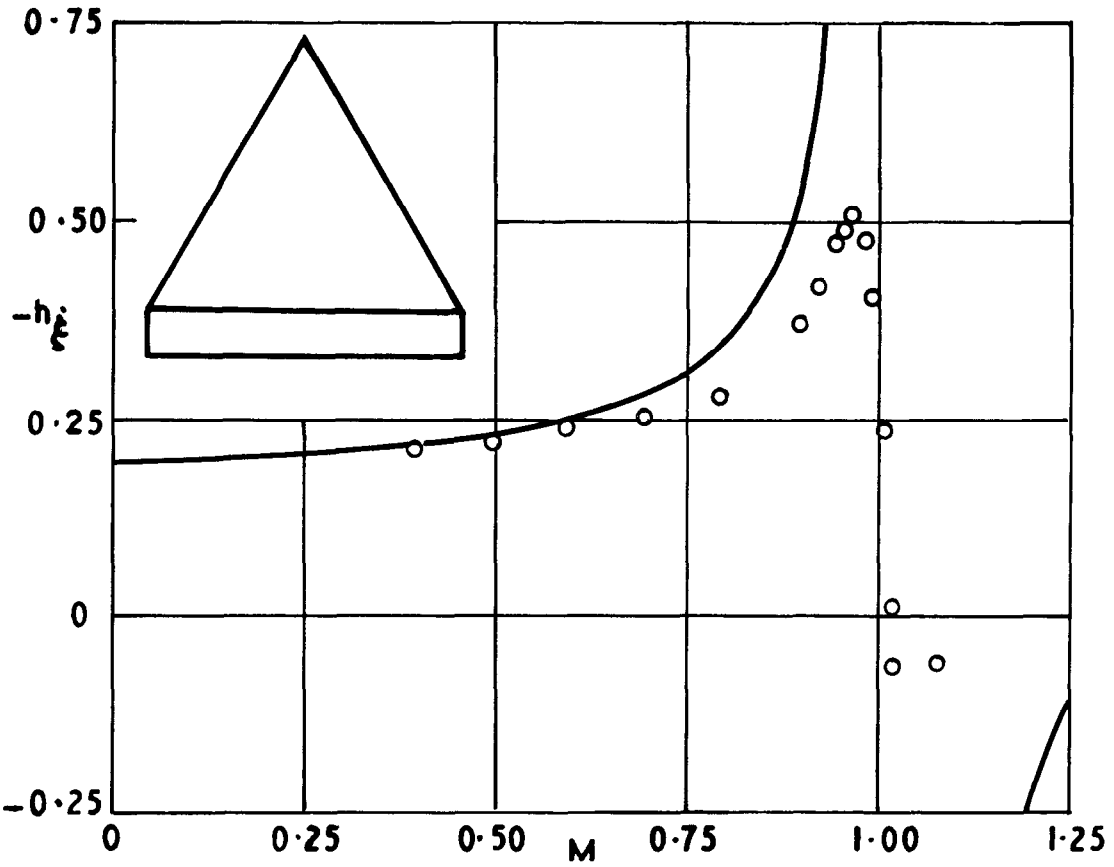

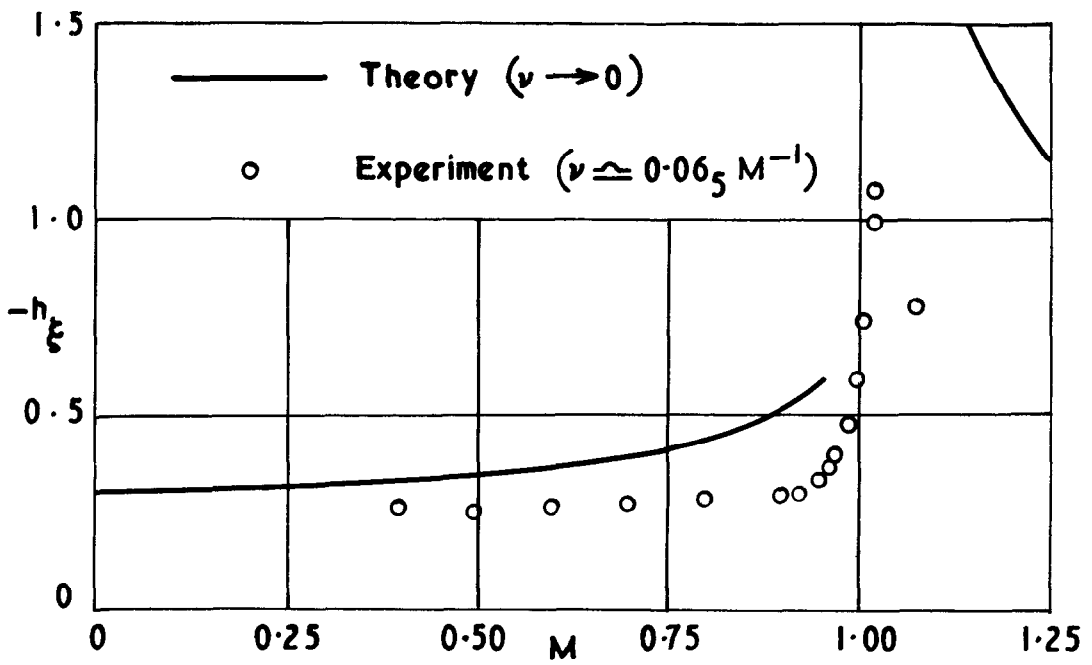

Hinge-moment derivatives against M for a delta wing (A = 1·8) with oscillating flap

FIG. 11

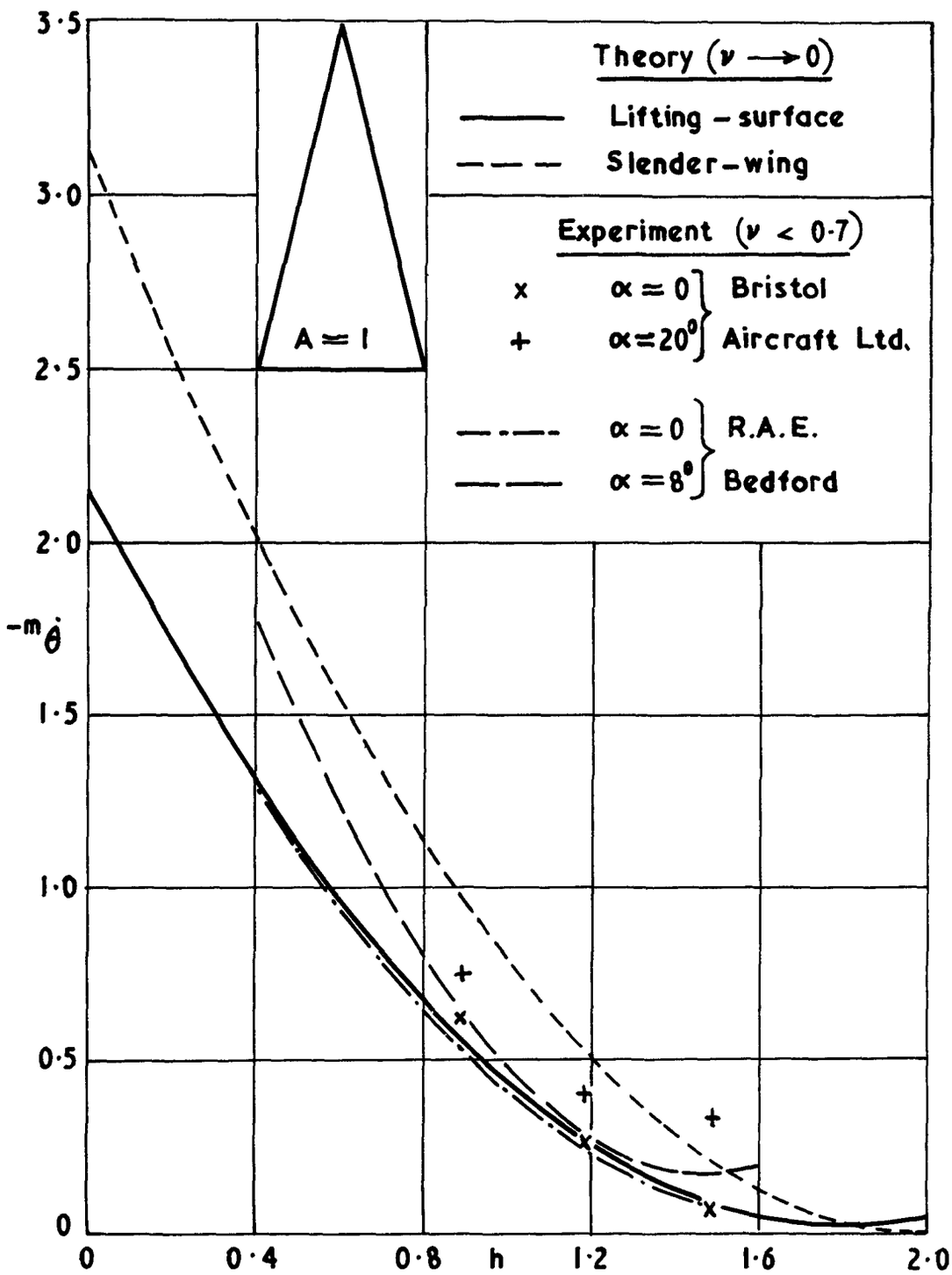

$-m_{\dot{\theta}}$ against h for a triangular wing (A = 1) at M = 0

FIG. 12.

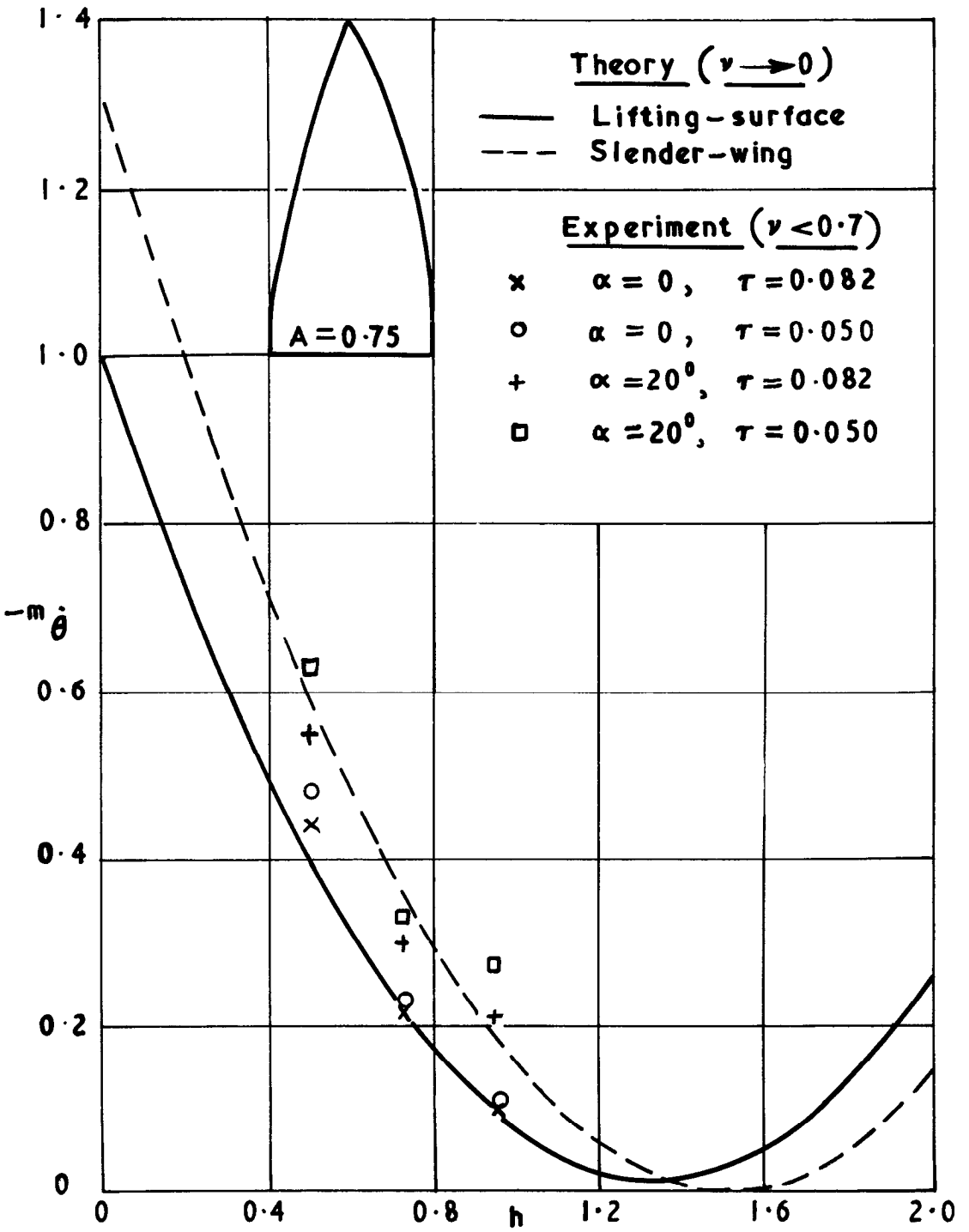

$-m_{\dot{\theta}}$ against h for gothic wings (A=0·75) at M=0

FIG. 13

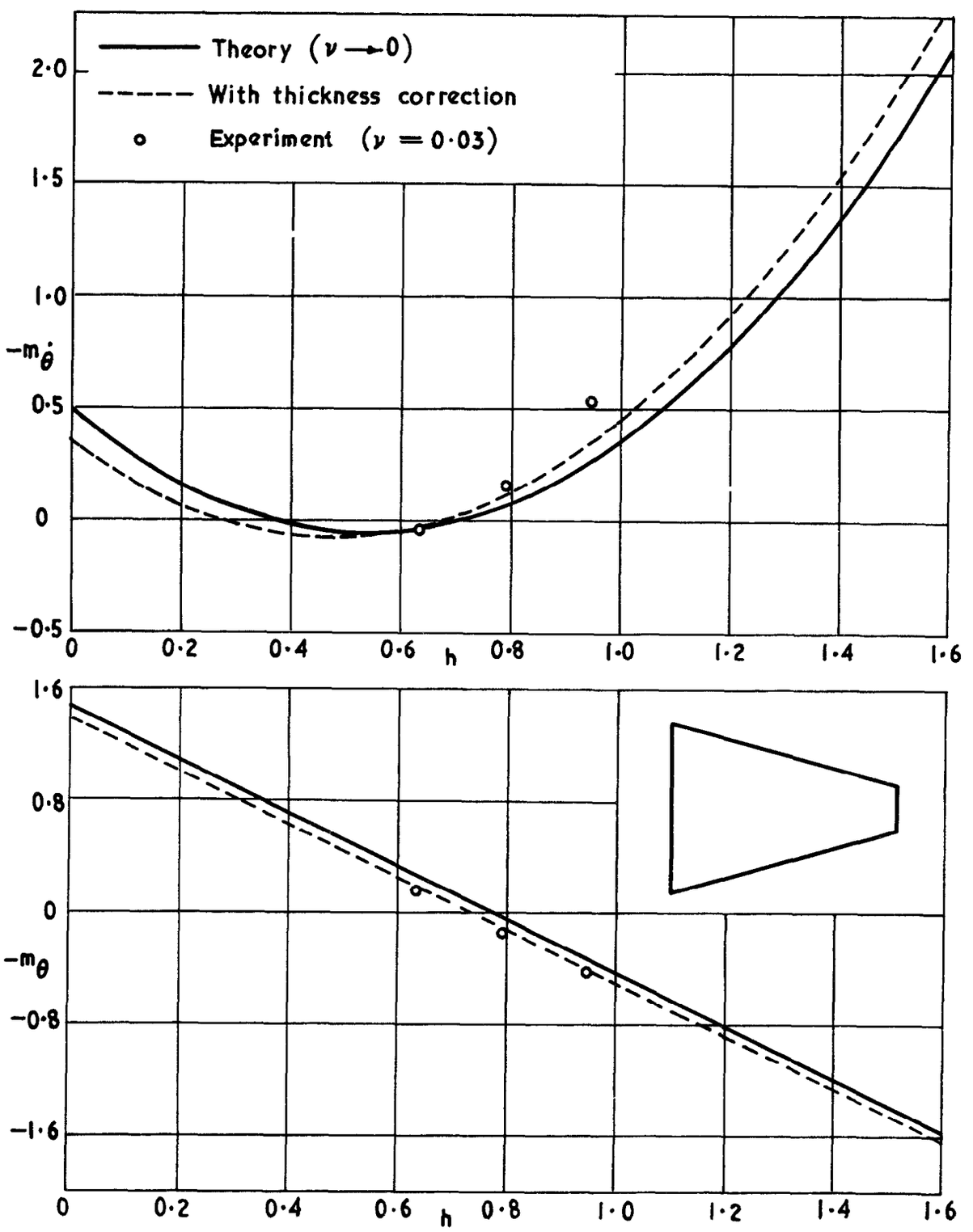

$-m_\theta$ and $-m_{\dot{\theta}}$ against h for thick tapered wing at $M = \sqrt{2}$

FIG. 14

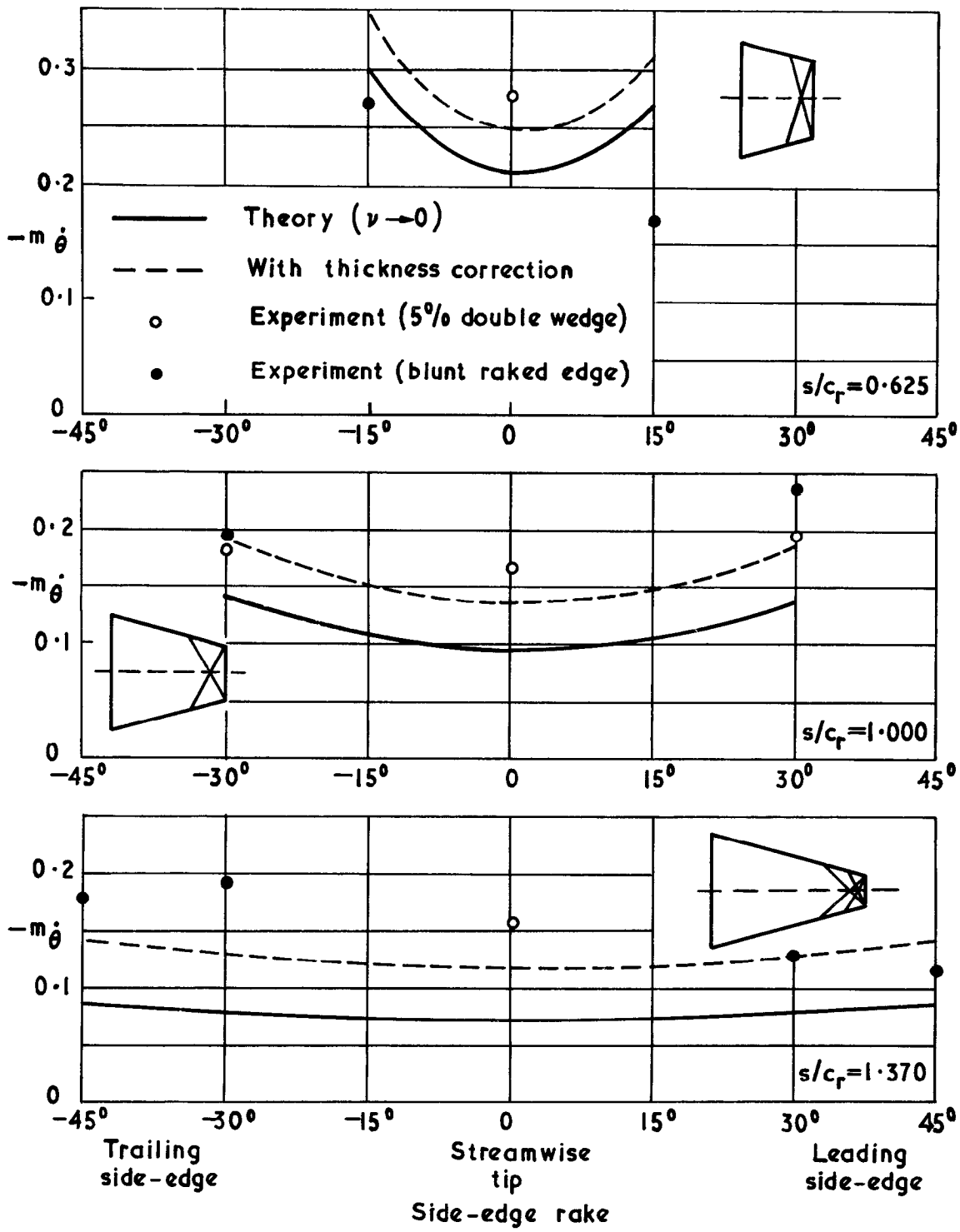

$-m_{\dot{\theta}}$ against side-edge rake for different spans of wing at $M=\sqrt{2}$

FIG.15

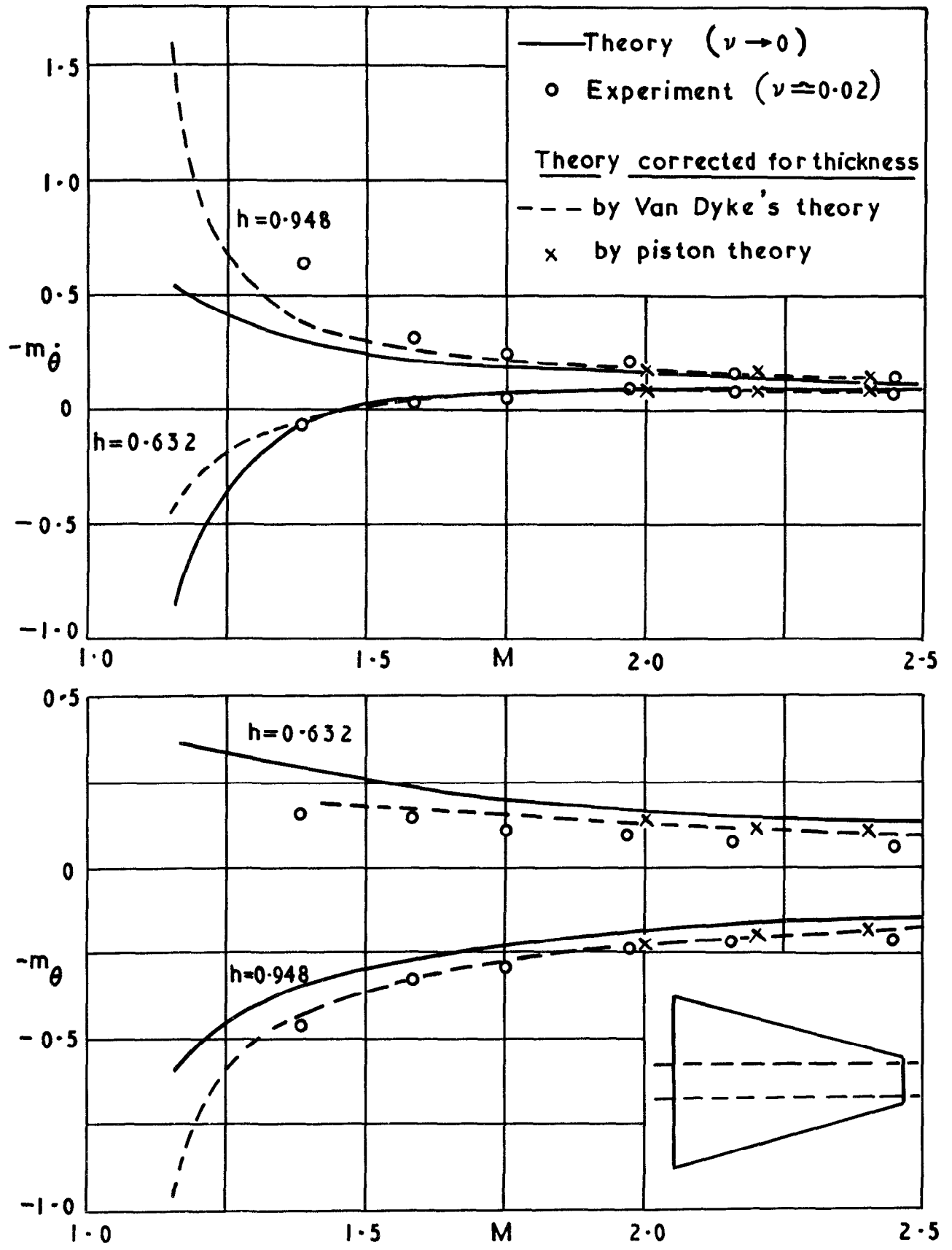

$-m_{\theta}$ and $-m_{\dot{\theta}}$ against M for thick tapered wing

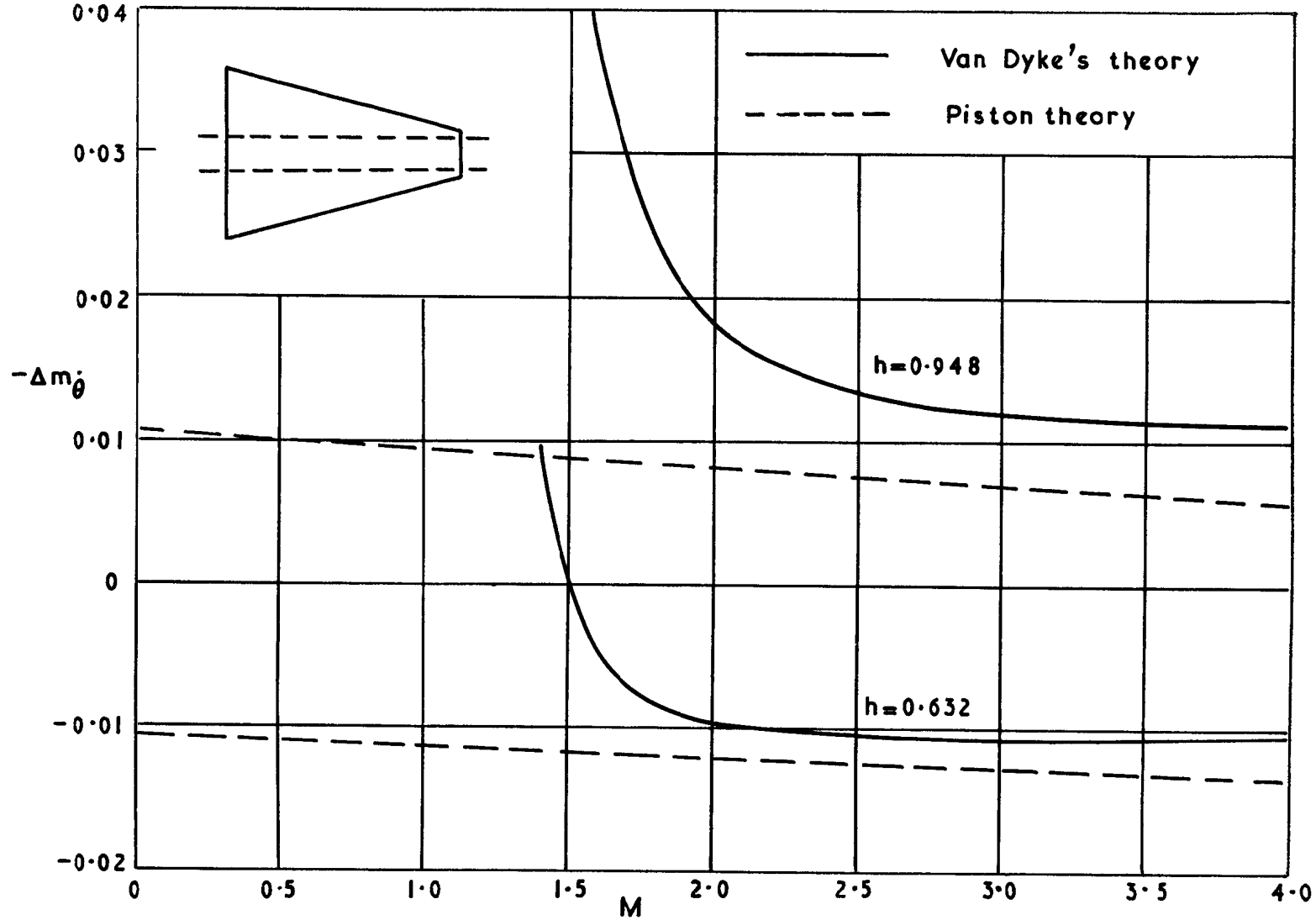

FIG.16

Incremental thickness corrections to $-m_{\dot{\theta}}$ for wing with 5% double-wedge section

FIG. 17

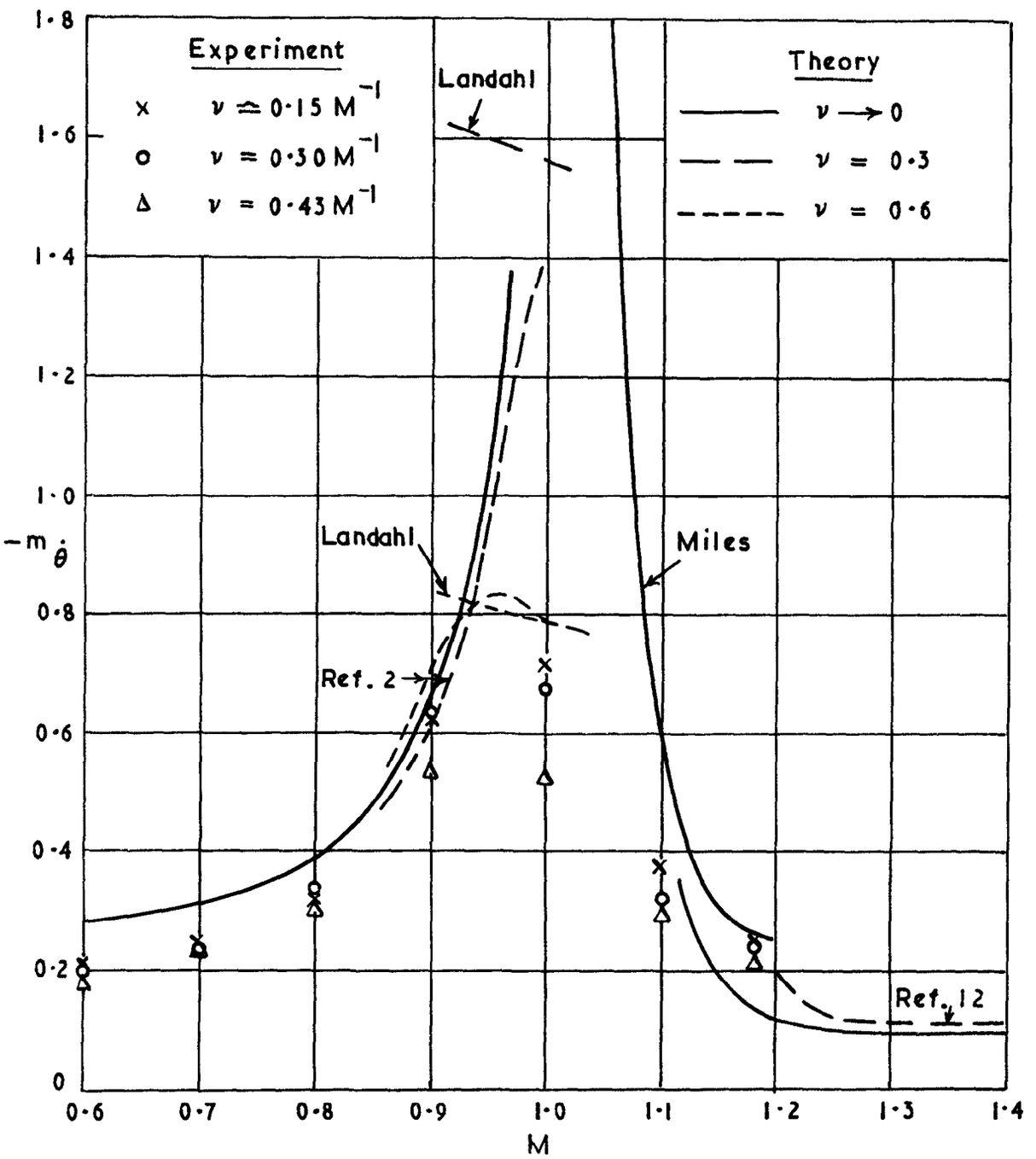

$-m_{\dot{\theta}}$ against M for rectangular wing (A = 2) with h = 0·42

FIG.18

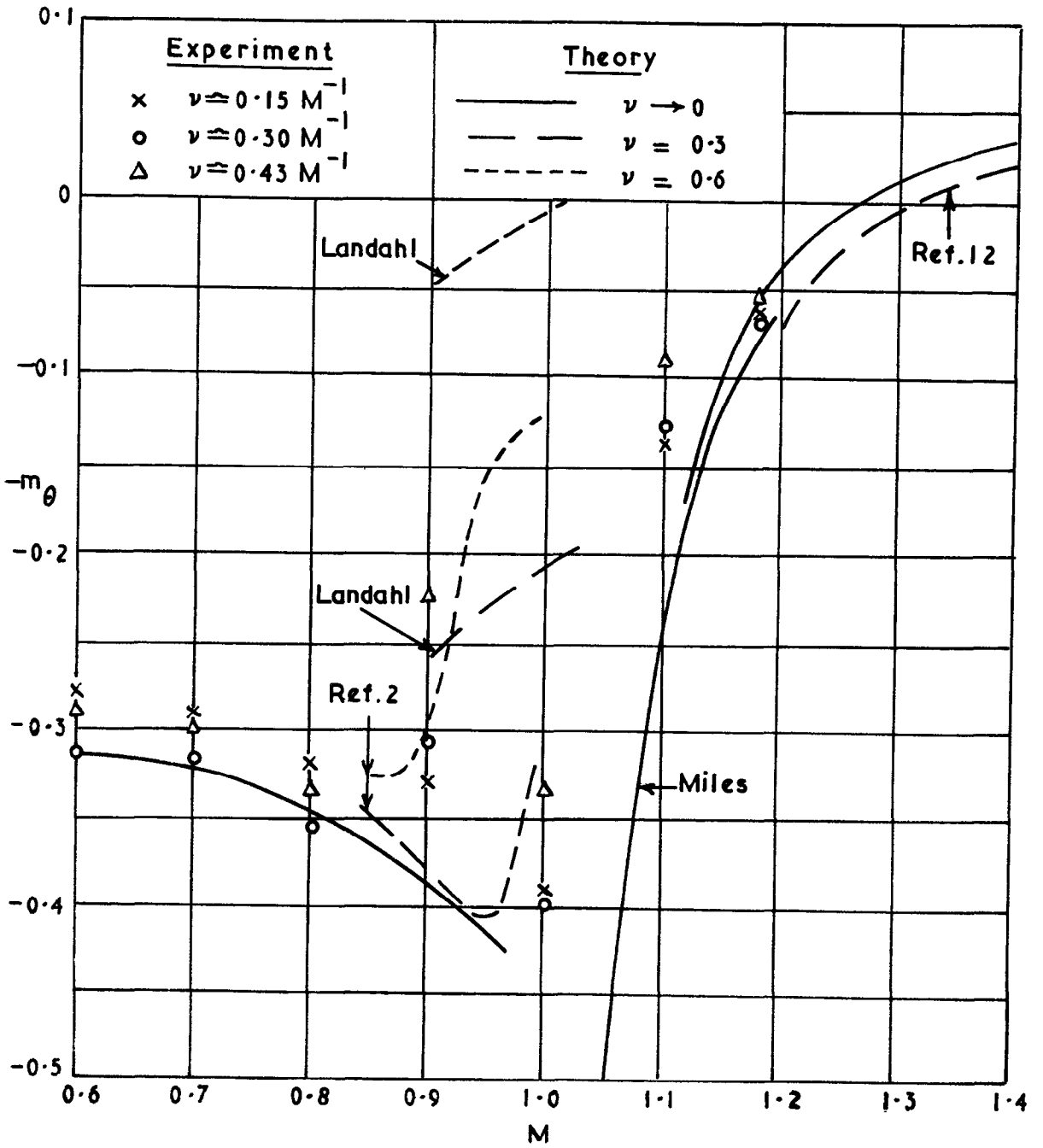

$-m_\theta$ against M for rectangular wing(A=2)with h=0·42

FIG. 19

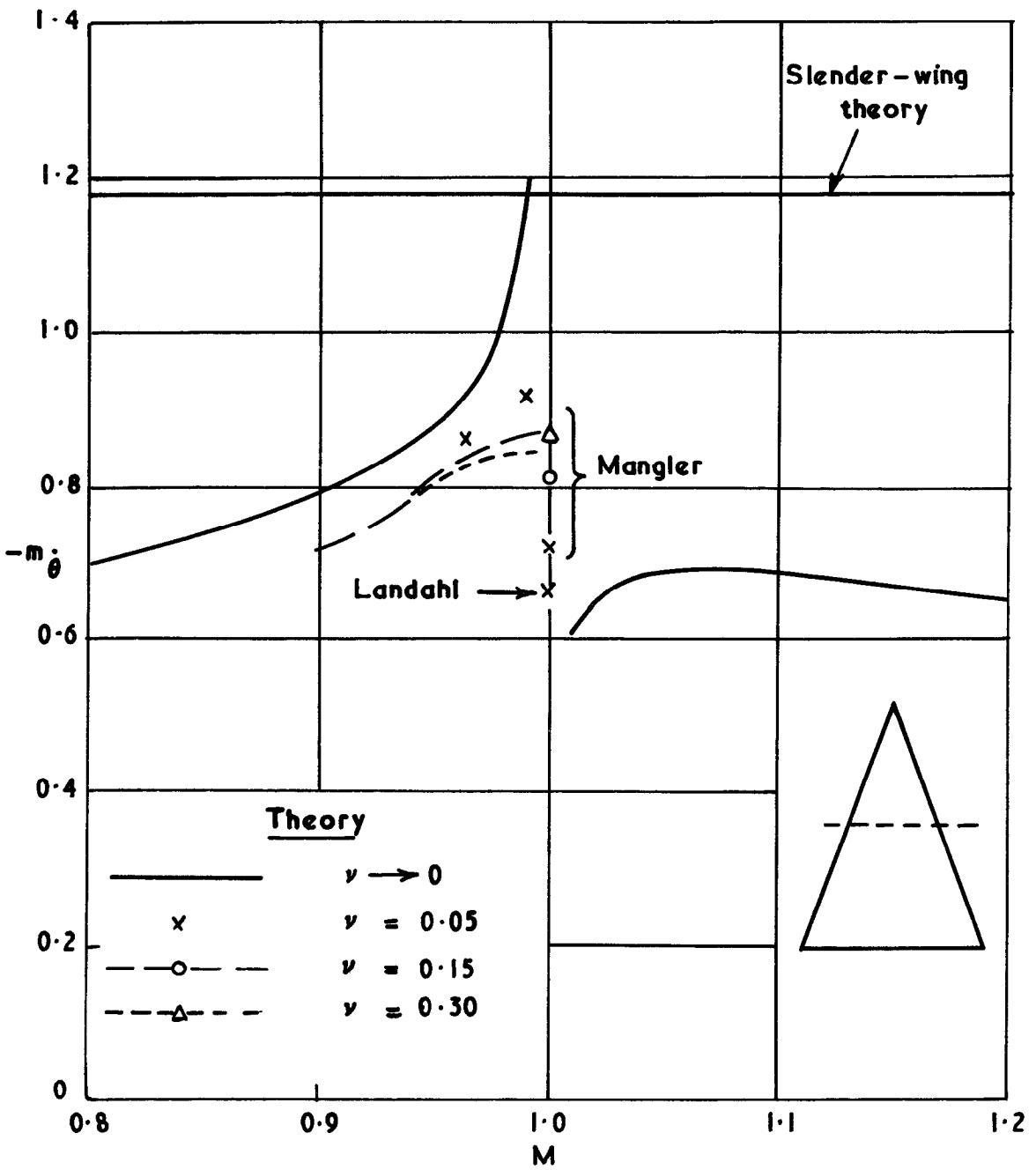

$-m_{\dot{\theta}}$ against M for a triangular wing (A = 1·5) oscillating about the half-root-chord axis

FIG.20

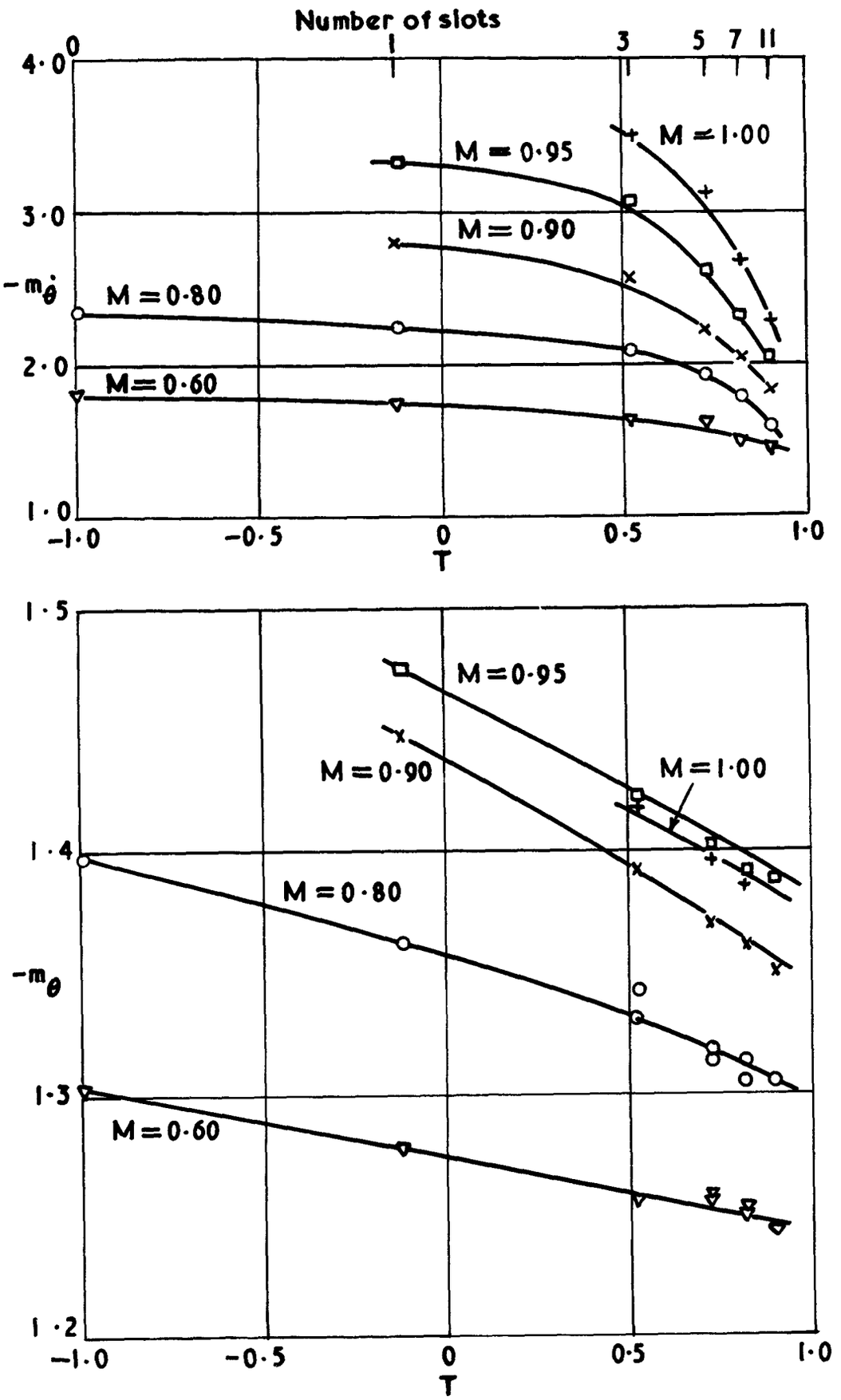

Effect of slot width and spacing on derivatives measured in a slotted-wall rectangular tunnel

FIG.21

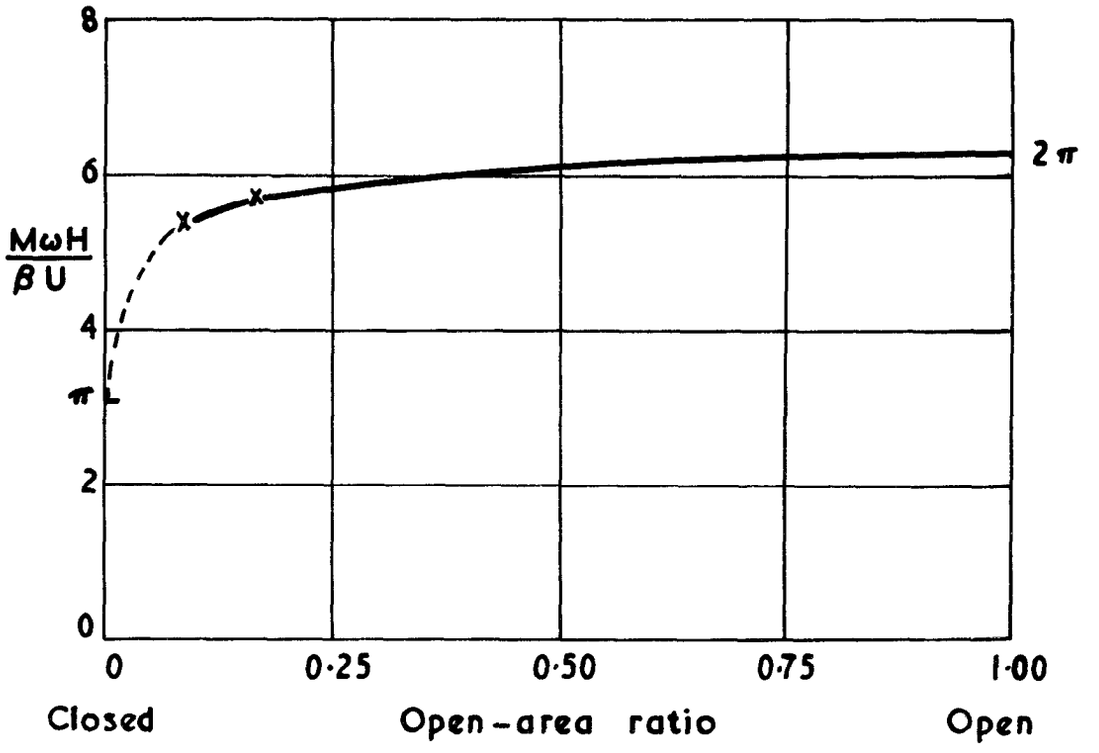

Critical frequency for resonance in rectangular tunnels with longitudinally slotted roofs and floors

A.R.C. C.P. No.623. March, 1961

Acum, W. E. A. and Garner, H. C.

THE ESTIMATION OF OSCILLATORY WING AND CONTROL DERIVATIVES

The paper reviews the accuracy of theoretical predictions of derivatives for wing and control oscillations and illustrates this by recent experimental work at Mach numbers between 0 and 2·5. The chief area of uncertainty is in the transonic flow regime, but further development is also required for slender wings and oscillatory interference in slotted-wall tunnels.

A.R.C. C.P. No.623. March, 1961

Acum, W. E. A. and Garner, H. C.

THE ESTIMATION OF OSCILLATORY WING AND CONTROL DERIVATIVES

The paper reviews the accuracy of theoretical predictions of derivatives for wing and control oscillations and illustrates this by recent experimental work at Mach numbers between 0 and 2·5. The chief area of uncertainty is in the transonic flow regime, but further development is also required for slender wings and oscillatory interference in slotted-wall tunnels.

A.R.C. C.P. No.623. March, 1961

Acum, W. E. A. and Garner, H. C.

THE ESTIMATION OF OSCILLATORY WING AND CONTROL DERIVATIVES

The paper reviews the accuracy of theoretical predictions of derivatives for wing and control oscillations and illustrates this by recent experimental work at Mach numbers between 0 and 2·5. The chief area of uncertainty is in the transonic flow regime, but further development is also required for slender wings and oscillatory interference in slotted-wall tunnels.

Printed and published by
HER MAJESTY'S STATIONERY OFFICE
To be purchased from
York House, Kingsway, London W.C.2
423 Oxford Street, London W.1
13A Castle Street, Edinburgh 2
109 St. Mary Street, Cardiff
39 King Street, Manchester 2
50 Fairfax Street, Bristol 1
35 Smallbrook, Ringway, Birmingham 5
80 Chichester Street, Belfast 1
or through any bookseller

Printed in England

S.O. Code No. 23-9013-23